EXPLORATORY INVESTIGATION OF SOUND PRESSURE LEVEL IN THE WAKE OF AN OSCILLATING AIRFOIL IN THE VICINITY OF STALL

By Robin B. Gray and G. Alvin Pierce
Georgia Institute of Technology
Atlanta, Georgia

Prepared for

NATIONAL AERONAUTICS AND SPACE ADMINISTRATION

NASA Langley Research Center
Grant NGR 11-002-121
John F. Ward, Project Manager

EXPLORATORY INVESTIGATION OF SOUND PRESSURE LEVEL IN THE WAKE OF AN OSCILLATING AIRFOIL IN THE VICINITY OF STALL

By Robin B. Gray and G. Alvin Pierce
Georgia Institute of Technology
Atlanta, Georgia

SUMMARY

Wind-tunnel tests were performed on two oscillating two-dimensional lifting surfaces. The first of these models had an NACA 0012 airfoil section while the second simulated the classical flat plate. Both of these models had a mean angle of attack of 12 degrees while being oscillated in pitch about their midchord with a double amplitude of 6 degrees. Wake surveys of sound pressure level were made over a frequency range from 16 to 32 Hz and at various free-stream velocities up to 100 ft/sec.

The sound pressure level spectrum indicated significant peaks in sound intensity at the oscillation frequency and its first harmonic near the wake of both models. From a comparison of these data with that of a sound-level meter, it is concluded that most of the sound intensity is contained within these peaks and no appreciable peaks occur at higher harmonics. It is concluded that within the wake the sound intensity is largely pseudosound while at one chord length outside the wake, it is largely true vortex sound. For both the airfoil and flat plate the peaks appear to be more strongly dependent upon the airspeed than on the oscillation frequency. Therefore reduced frequency does not appear to be a significant parameter in the generation of wake sound intensity.

INTRODUCTION

One of the most significant operational deficiencies of a helicopter is the extreme noise environment which it generates. The physical

phenomenon behind this intense source of acoustical energy has been open to question and debate for a long period of time. One hypothesis is that the strong harmonic vorticity shed by the retreating blade while it is in the vicinity of stall is a prime contributor to the noise environment. If this is true it is necessary that a fundamental knowledge be obtained of such an acoustical environment and of the parameters which influence this environment.

In an effort to simulate an oscillating rotor blade near the condition of stall, a wind-tunnel investigation has been conducted on two oscillating two-dimensional lifting surfaces. Although the unsteady two-dimensional flow field is a poor approximation to the complex three-dimensional flow behind an actual rotor, it does isolate the basic phenomena associated with pure dynamic stall. The tests were conducted at a mean angle of attack corresponding to the static stall angle. For a fixed amplitude of oscillation about the midchord the spectum of sound pressure level was recorded throughout the wake. These measurements were made for a broad range of frequency and airspeed.

SYMBOLS

c	airfoil chord, feet
f	frequency of oscillation, Hertz
p	pressure, dynes per centimeter^2
q	free-stream dynamic pressure, dynes per centimeter^2
SPL	sound pressure level, $20 \log_{10} \frac{p}{0.0002}$
V	free-stream velocity, feet per second
x	downstream distance from airfoil midchord, feet
z	vertical distance above airfoil midchord, feet
α	airfoil mean angle of attack, degrees
$\Delta\alpha$	single amplitude of airfoil oscillation, degrees

APPARATUS AND TESTS

This test program was conducted in the 9-ft Georgia Tech low-speed wind tunnel. Two-dimensional flow was simulated about an oscillating airfoil as illustrated in figure 1. This airfoil was oscillated by a drive mechanism contained in one of the wind screens shown in the figure. Free-stream velocity was determined from the floor-mounted pitot which had been calibrated to the true airspeed at the airfoil midchord.

Drive Mechanism

A one horsepower variable speed motor was used to drive an eccentric pinion which transmitted a pitching oscillation to the airfoil through a linkage system. The linkage was designed to produce a model angle-of-attack change of ± 3 degrees about steady mean angles from 7 to 15 degrees. There was no mechanical contact between the drive mechanism plus model and the wind tunnel plus wind screens. This permitted static lift measurements to be made when the drive mechanism was mounted on the electro-mechanical balance beneath the tunnel. When the model was oscillated the drive mechanism was mounted to the building foundation. This procedure eliminated unwanted mechanical vibrations from being transmitted to the tunnel and wind screens.

The wind screens which enclosed the drive mechanism were mounted to the tunnel floor as seen in figure 1. These fairings were intended to produce a nearly two-dimensional flow about the model. They projected one and a half chord lengths above the airfoil which was two and a half chord lengths above the tunnel floor. The screens extended one chord length forward of the leading edge and aft of the trailing edge.

The supporting structure for the drive linkage was completely lined with one-inch thick fiber glass to deter unwanted sound from being transmitted to the wind screen and in turn to the air stream.

Models

The primary model for the test program had an NACA 0012 airfoil section with a constant chord of 12 inches and a span of 28 inches. This model was constructed of laminated balsa which was cemented to a quarter-inch thick aluminum plate which extended over approximately half the chord. The aluminum plate had numerous holes drilled through it to minimize the mass moment of inertia about the axis of rotation. This axis was the midchord of the airfoil.

A second model which was utilized in the test program was intended to simulate the classical flat plate approximation of thin airfoil theory. This configuration consisted of a solid quarter-inch flat aluminum plate with a chord of 12 inches and a span of 28 inches. Both the leading and trailing edges were rounded to an eighth-inch radius, and the axis of rotation was again at the midchord.

Instrumentation

A Brüel and Kjaer one-inch condenser microphone (Model 4144) was used to survey the sound pressure level in the wake of the oscillating models. This microphone was mounted at the closed end of a quarter-inch diameter aluminum tube of 8 inches length. The tube was aligned with the free stream such that its open end was upstream. The resonant frequency of the open-ended tube was much above the frequency range of interest. The microphone-tube assembly was mounted on a vertical traversing mechanism as illustrated in figure 1. Although it was possible to remotely traverse the wake vertically, it was necessary to shut the tunnel down to change the streamwise position of the mechanism.

The output of the microphone was processed on line as illustrated by the flow chart of figure 2. The microphone output was appropriately amplified by a Brüel and Kjaer microphone amplifier (Model 2604) before being filtered and averaged by a Spectral Dynamics dynamic analyzer (Model SD 101B). This tracking filter utilized a 1.5 Hz bandpass filter which was centered by a Spectral Dynamics sweep oscillator (Model SD 104A).

The logarithm of the sine average of the filtered signal, which represented the sound pressure level as obtained from the tracking filter, was then recorded on an X-Y plotter versus frequency from the sweep oscillator.

The absolute value of sound pressure level was determined using a Dynasciences acoustic calibrator (Model PC-125). The calibrator was mounted at the open end of the microphone tube, and for various sound pressure levels at 1000 Hz the sine-averaged filtered signal was used to calibrate the X-Y plotter.

An accurate measurement of the oscillation frequency of the model was obtained by placing a magnetic pick-up near the 16-cog driven gear of the motor drive mechanism. This transducer produced 16 pulses per cycle of model motion which was then counted by a Monsanto electronic counter (Model 104A). Thus the driving frequency of the model could be regulated to within approximately a quarter Hz.

Test Program

The initial test consisted of making a velocity survey in the vertical center plane between the wind screens to ascertain the uniformity of the flow. Subsequently both the NACA 0012 airfoil and flat plate models were installed to obtain their static lift characteristics. For these static measurements the entire drive mechanism was mounted on the six-component electro-mechanical balance of the 9-ft tunnel.

The primary portion of the test program consisted of measuring the sound pressure level in the wake of the two models. With the drive mechanism mounted to the building foundation the models were oscillated in pitch about their midchord. These oscillations had a double amplitude of 6 degrees about a mean angle of attack of 12 degrees. The measurements were made over a range of frequency from 16 to 32 Hz and at various free-stream velocities up to 100 ft/sec.

RESULTS AND DISCUSSION

The results are presented in four sections: Velocity Survey, Static Lift Data, Airfoil Wake Measurements, and Flat Plate Wake Measurements.

The airfoil support structure and drive mechanism were installed in fairings mounted on the tunnel floor in order to minimize their effect on the flow field and to reduce the noise level attributable to the drive mechanism. The fairings did not extend completely across the test section but terminated six inches above the centerline as a compromise between tunnel blockage and maintaining nearly two-dimensional flow at the airfoil location. A reasonable compromise was obtained. Sound pressure level measurements taken with the airfoil removed, tunnel on, and drive mechanism running showed that no discrete frequency peaks appeared above the overall sound level at all test speeds and drive frequencies.

Since the wake sound pressure levels were obtained with a sensitive microphone, both true sound pressure and "pseudosound" pressure were measured. The former is associated with the compressibility of air and the propagation of pressure waves at the local speed of sound. The latter arises from pressure fields moving with the local airspeed such as those associated with vortex streets. If both are present, it is not possible to distinguish between their individual contributions to the measured "sound" levels. However, the intensity of true vortex noise is approximately proportional to the sixth power of the velocity whereas pseudosound is proportional to the fourth power (Chapter IV, reference 1). This permits some judgement to be reached as to the major source of the levels measured.

In the results and discussions that follow, the term"sound pressure level" is used to refer to both cases.

Velocity Survey

The results of a velocity survey made in the longitudinal centerline plane, airfoil removed, with a pitot-static tube is shown in figure 3 for the case of 150 ft/sec at the airfoil midchord point (also the axis of oscillation). The survey covered an area one chord length above and below and one-half chord length ahead and three chord lengths behind the midchord point. Surveys were also made for 50 and 100 ft/sec. The results were very similar in all three cases.

The lines of constant per cent difference from the velocity at the airfoil midchord position are shown. In the streamwise direction along the airfoil chord location, the effective velocity varies from one per cent lower at the leading edge to one-half per cent lower at the trailing edge. Along the vertical axis at the midchord, the velocity is one per cent lower at one-half chord length above the midchord and increases to one-half per cent higher at one-half chord length below. This variation would appear to be acceptable for the purposes of this study.

The downstream variation is attributable to the blockage effect of the fairings. It is to be noted that the velocity variation across the vertical centerline plane along the survey traverse lines is small except for the rearmost line. Thus sound pressure level comparisons along a vertical survey line should be good but there may be unknown effects in the streamwise comparisons.

Static Lift Data

Static lift coefficient as a function of angle of attack at 50, 100, and 150 ft/sec is presented in figure 4 for the NACA 0012 airfoil and in figure 5 for the flat plate airfoil. The results compare acceptably with two-dimensional data available in the literature for both cases (reference 2). However, the lift curve slopes for the NACA 0012 airfoil are slightly lower and the maximum lift coefficients are about ten per cent lower than the published data at approximately the same Reynolds number. Angle of attack for maximum lift is in good agreement. The differences are attributed to the 1/4-inch gap between the airfoil and the fairings.

Airfoil Wake Measurements

Figure 6 is a sample plot of the sound pressure level (SPL) data as a function of frequency at an effective airspeed of 100 ft/sec and an oscillation frequency of 24 Hz. The data presented in figures 7 through 16 were obtained from similar plots from which the peak levels were read at the corresponding fundamental and first harmonic frequency of oscillation. In many cases, discrete peaks were obtained but in several

cases both inside and outside of the wake no peaks were discernible, particularly at the low speeds. In these cases, the overall noise level at the particular fundamental and first harmonic frequency of oscillation was read and plotted.

Figures 7 through 11 show the variation across the wake of the first peak sound pressure level at five different oscillation frequencies (16, 20, 24, 28, and 32 Hz) each at five different tunnel velocities (0, 25, 50, 75, and 100 ft/sec) at one chord length downstream of the trailing edge. For oscillation frequencies of 16, 24, and 32 Hz, data are also presented for two and three chord lengths downstream at 0, 25, and 100 ft/sec. Arrows are used to help identify sequentially the downstream survey data. Data points with a hash mark represent check runs.

With the tunnel off, the measurements represent true sound levels and as would be expected, the sound intensity generally increases with increasing frequency and decreases with increasing distance from the airfoil. The variations along the survey lines are most probably due to interactions of the waves from the oscillating airfoil and/or reflected waves from the fairings and wind tunnel walls. The orientation of the microphone may also have an effect.

At one chord length downstream and for any given frequency, an increase in airspeed has associated with it an increase in peak SPL. The data indicate that the increase in SPL is more strongly dependent on airspeed than on oscillation frequency.

In figure 7 for 16 Hz and at 25 ft/sec, a bucket begins to develop in the peak SPL at two chord lengths downstream with an additional 17 db reduction at three chord lengths. Outside of this bucket, the changes are much smaller. In figure 9 for 24 Hz and the same speed, a bucket appears at the two chord length station but no further reduction occurs downstream. In figure 11 for 32 Hz, there is relatively little change within the wake at two chord lengths downstream, and a relatively large change at three chord lengths. The causes for this behavior are not apparent.

The data in the same figures for 100 ft/sec are much more consistent.

At two chord lengths downstream a bucket has developed in the peak SPL and the reduction is approximately the same for all three frequencies amounting to 15-18 db. At three chord lengths downstream, the bucket has essentially disappeared and the peak SPL is only 3 to 6 db below that at one chord length. In all cases, the peaks and buckets are approximately located where the centerline of the wake would be expected to be. This downstream variation in SPL is also not explained. A maximum SPL of 144 db was measured at one chord length downstream for all frequencies above 16 Hz.

Figures 12 through 16 show the variation across the wake of the second peak sound pressure level at the first harmonic of the five oscillation frequencies (16, 20, 24, 28, and 32 Hz) each at the five tunnel velocities (0, 25, 50, 75, and 100 ft/sec) at one chord length downstream of the trailing edge. For oscillation frequencies of 16, 24, and 32 Hz, data are also presented for two and three chord lengths downstream at 0, 25, and 100 ft/sec. Arrows are again used to help identify sequentially the downstream survey data. Data points with a hash mark represent check runs.

With the tunnel off, the measurements again represent true sound levels. At 16 Hz, the SPL is low being only slightly higher than the threshold of the microphone sensitivity and showing very little variation along the survey lines or with downstream distance. The highest values were measured at 20 Hz but again with relatively little variation along the survey line. At 24 Hz, the SPL is lower, some variation is observed along the survey line, and depending upon vertical location, the level increases or decreases with downstream distance. At 28 Hz, a peak is present with a 10 db variation along the survey line. At 32 Hz, there is a smaller variation along the survey line with the levels generally increasing with distance in the downstream direction. These results may also be due to wave interactions and perhaps some structural resonances in the tunnel test section or fairings.

With the tunnel on and for any given frequency at one chord length downstream, peak SPL increases with airspeed. As was noted for the first peak, the data indicate that this increase is more strongly dependent on airspeed than on frequency. In general, it appears that for any given

frequency, the wake width as determined by the SPL measurements decreases with increasing speed. This may be a Reynolds number effect. There is some indication that the maximum SPL at any given airspeed occurs in the vicinity of an oscillation frequency of 20 Hz, although as for the first peak, there is not much change in maximum SPL with frequency at constant speed.

In figure 12 for 16 Hz and 25 ft/sec, the maximum SPL increases by 4 db at two chord lengths downstream with a decrease of 2 db at three chord lengths. The wake width as determined by the SPL measurements also decreases with increasing distance. In figure 14 for 24 Hz and the same tunnel speed, the maximum SPL has decreased by 5 db at two chord lengths downstream and has decreased another 5 db at three chord lengths. The apparent wake center has shifted downward and its width has increased somewhat. In figure 16 for 32 Hz, the variation is like that at 16 Hz.

In the same figures at 100 ft/sec, the wake width increases with downstream location with a definite downward shift in maximum SPL position between two and three chord lengths downstream. The maximum SPL increases by 4 to 9 db between one and two chord lengths downstream and decreases by 4 to 7 db between two and three chord lengths, the largest increase occurring for 32 Hz and the largest decrease for 24 Hz. The maximum SPL of 142 db was measured at two chord lengths downstream for a 32 Hz oscillation frequency.

Sound pressure levels were also measured with a sound-level meter covering a range from 2 to 7000 Hz. This was done to check against the possibility that one or more relatively large peaks in SPL might exist at harmonic frequencies higher than the first. These overall sound pressure levels would be expected to be somewhat higher than those determined at the discrete frequencies from the tracking filter. Figure 17 shows the SPL distribution at one chord length downstream for no oscillation of the airfoil. Except for the 25 ft/sec case, the wakes are much narrower than with the airfoil oscillating although the peak SPLs are very little different from the corresponding oscillating case. The large width for the 25 ft/sec case may be due to the effect of Reynolds number on the stall characteristics of the airfoil. The dashed line indicates what

might be expected without this effect.

Figure 18 presents the overall sound pressure levels at one chord length downstream for all frequencies of oscillation. The objective here is to show the range of SPL measured by the sound-level meter for comparison with the distributions of the fundamental frequencies of figures 7 through 11. It is concluded that the comparison is good, being somewhat better at the higher frequencies.

It was pointed out earlier that since the microphone is a fluctuating-pressure-measuring device, it is not possible to separate true sound pressure from pseudosound pressure. The basic definitions of sound are in terms of the magnitude of the fluctuating component of pressure in a fluid medium and the sound pressure level is defined as

$$SPL = 20 \log_{10} \frac{p}{0.0002}$$

where 0.0002 dynes/cm^2 is an accepted standard reference value against which other pressures, p, are compared.

In this study, it would be expected that the true sound of interest would be that associated with the fluctuating pressures on the surface of the oscillating airfoil which in turn lead to vortex shedding into the wake. An analysis of the vortex sound phenomenon in Chapter IV of reference 1 shows that the vortex sound intensity is proportional to V^{2n} where the factor of proportionality is a function of Reynolds number, the body geometry, the orientation of the microphone, and the characteristics of the fluid medium. Analysis and experiment show that the exponent, n, should be about 3 for vortex sound.

Now considering the shed vortex street itself, a microphone fixed in space relative to the moving stream would detect a fluctuating pressure with the passage of the vortex elements of the street. However this fluctuating pressure should be proportional to the velocity squared and the corresponding pseudosound intensity measured by the microphone should be proportional to the fourth power of the velocity. Thus for vortex sound and pseudosound, the above definition may be written as

$$SPL = 20 \log_{10} \frac{c\, V^n}{0.0002}$$

where n should be about 3 for true vortex sound and 2 for pseudosound. Therefore if SPL and velocity are plotted on semi-logarithmic graph paper, the slope of the line joining the points will be the exponent, n, in the above definition.

In figure 19, peak SPL at the fundamental frequency is plotted as a function of velocity for the microphone located at z/c = - 0.25; x/c = 1.0. The effective SPL of the tunnel dynamic head, q, is plotted as a reference line having a slope of 2. A straight line having the same slope is drawn through the data points as shown in the figure. It is concluded that the data measured are largely pseudosound.

In figure 20, peak SPL at the first harmonic of the fundamental frequency is plotted as above for the same location. Again it may be concluded that the data measured are largely pseudosound.

In figure 21, the SPL at the fundamental frequency is plotted for the microphone located at z/c = 1.0; x/c = 1.0. Straight lines having slopes of 2, 2.5, and 3 are drawn for reference and it may be concluded that for airspeeds greater than 50 ft/sec, the measured data are largely true vortex sound.

In figure 22, the SPL at the fundamental frequency is plotted for the microphone located at z/c = -1.0; x/c = 1.0. Straight lines having slopes of 2, 2.5, and 3 are drawn for reference and no definite conclusions may be reached. Since this location is closer to the test section floor, the reflections may be affecting the measured data.

In figure 23, the more limited SPL data at the first harmonic of the fundamental frequency are plotted for the microphone located at z/c = - 0.25 and two and three chord lengths downstream. It appears that the measured data are again pseudosound.

The peak SPL at the fundamental frequency is shown in figure 24 at one chord length downstream as a function of reduced frequency, $\pi fc/V$, which is also approximately ten times the reduced Strouhal frequency,

$(2\pi fc \sin \alpha)/V$. The solid lines represent the variation at constant tunnel velocity and the dashed lines, at constant frequency of oscillation. As pointed out before, the peak SPL appears to be largely a function of the tunnel velocity for the range of variables covered. For any given velocity above 50 ft/sec, the maximum SPL occurs near an oscillation frequency of 28 Hz. As far as this is concerned, there does not appear to be an obvious dependency on reduced frequency. The different behavior of the data at 25 ft/sec is not explained.

The peak SPL at the first harmonic of the fundamental frequency is shown in figure 25 at one chord length downstream as a function of the reduced frequency. The solid lines represent the variation at constant tunnel velocity. Due to the scatter of the data points, the lines of constant oscillation frequency were not drawn. Again, the SPL is seen to have a larger variation with tunnel speed than with the frequency of oscillation. It appears that the maximum SPL at all of the tunnel speeds tested occurs near 20 Hz. Again there does not appear to be an obvious dependency on reduced frequency.

Flat Plate Wake Measurements

A representative test condition was chosen for determining the sound pressure levels in the wake of an oscillating flat plate airfoil. The primary purpose for this test was for comparison with the NACA 0012 airfoil results in order to determine the validity of the flat plate model for calculating thick-airfoil wake characteristics. The flat plate was set at a mean angle of attack of 12° with an oscillation amplitude of 3° and a frequency of 20 Hz. Tests were run at 0, 25, and 50 ft/sec and measurements were taken at 1, 2, and 3 chord lengths downstream of the trailing edge. The results are shown in figure 26 for the peak sound pressure level at 20 Hz and in figure 27 for the peak SPL at 40 Hz, the first harmonic of the fundamental frequency. The SPL versus frequency plots from which this data were obtained are similar in character to that of the airfoil in figure 6.

From a comparison of figure 26 and figure 8 at 50 ft/sec, the peak

SPL at 20 Hz for both is about 133 db at one chord length downstream but the wake width within which the level is above 130 db is about twice as wide for the flat plate as for the airfoil. At 25 ft/sec, the peak flat plate level is about 8 db below that of the airfoil and from the limited data, no comparison can be made on the width of the wake. At zero ft/sec, the flat plate does not show much variation whereas the airfoil has a sound reduction of 16 db in the region below the z = 0 plane. At two chord lengths downstream, the 25 ft/sec data have a noise level depression or bucket which does not show up in the 50 ft/sec data. This is not consistent with the airfoil data at other frequencies in which the depression at the lower speeds carries through to the higher speeds. The data at three chord lengths downstream are somewhat more consistent in that the level is several db below the one chord length data.

From a comparison of figure 27 and figure 13 at 50 ft/sec, the peak SPL at 40 Hz (twice the oscillation frequency) for both is about 125 db at one chord length downstream but the wake width within which the level is above 120 db is about three times as wide for the flat plate as for the airfoil. The flat plate data have a noise depression in the z = 0 plane. At 25 ft/sec, the peak flat plate level is again about 8 db below that of the airfoil. At zero ft/sec, the airfoil does not show much variation while the flat plate data are erratic and difficult to reproduce. At two chord lengths downstream, the data at 25 ft/sec are inconclusive while at 50 ft/sec, the sound bucket is at a lower position in the wake and down about 6 db. Further reductions in sound level occur in passing to three chord lengths downstream.

To further investigate the flow field, smoke was introduced into the stream ahead of the flat plate at several different spanwise stations. The smoke patterns were illuminated by a strobe light set at a flashing rate equal to the oscillation frequency. When the smoke was introduced at mid span, it was observed from above that the smoke passed straight downstream in the tunnel vertical centerline plane. When viewed from the side, the alternately shed vortices were plainly visible and their frequency was the same as that of the flat plate oscillation. In addition, it was observed that at one chord length aft of the trailing edge the wake

was approximately one chord length thick which is in agreement with figures 26 and 27. The wake also grew thicker as it passed downstream. Smoke was also introduced into the flow ahead of the flat plate at several vertical stations adjacent to the fairings. The smoke streamer remained attached to the fairing until about two inches ahead of its trailing edge where it separated. In the vicinity of the flat plate it was rapidly diffused and could not be observed.

From the limited amount of data, it appears that the flat plate may not be a good model for calculating the wake characteristics of a thick airfoil. However, the flat plate tested did not have a sharp trailing edge. Any further tests should include a configuration with a sharp trailing edge.

Additional tests were performed covering a range of oscillation frequencies from 10 to 23 Hertz. The microphone was positioned in the wake at one chord length aft of the trailing edge of the plate. In many of the tests, the frequency range covered by the X-Y plotter was increased. One such plot is shown as figure 28 in which SPL peaks in the wake are observed up to the fourth harmonic of the fundamental frequency of 14 Hertz. There appeared to be some dependence on frequency but no trend could be established. In some cases there would be peaks only at the fundamental frequency inside the wake while first, second, and even third would appear in the data taken below the wake. In other cases there would be higher harmonic peaks inside the wake but not outside. In all cases without oscillation, no peaks could be distinguished in the sound pressure levels either within or outside of the wake although the plate was certainly stalled. In comparing the data within the wake for the plate oscillating or static, it was generally observed that the noise level was higher in the static case by as much as 15 db or approximately equal to the peak SPL at the fundamental frequency of the corresponding oscillating plate. As an example, if the fundamental peak was at 110 db with the corresponding noise level at 95 db with the airfoil oscillating, the noise level for the static plate would be near 110 db at the same frequency. Outside of the wake however, the noise levels were very nearly the same for all frequencies including the static case. It would appear as if within the wake, the

oscillating plate were concentrating the turbulence about the frequency of oscillation without changing the overall sound pressure level.

In order to check the repeatability of the data, a rerun at 0 and 50 ft/sec and 20 Hz at two chord lengths downstream from the trailing edge was made. These data are plotted in figures 26 and 27 with the hash mark. The repeatability at 50 ft/sec was reasonably good but there was considerable scatter at 0 ft/sec.

CONCLUDING REMARKS

Considering the compromises required in the wind-tunnel installation, a reasonable approximation of two-dimensional flow was obtained in the vicinity of the airfoil and the lift data compared reasonably well with published data.

From a study of the sound pressure levels (SPL) measured over the ranges of effective airspeeds and oscillation frequencies covered and with the airfoil set at a mean angle of attack of 12°, the following remarks may be made:

For both the flat plate and the airfoil, the first and second peak SPL sppear to be more strongly dependent upon the airspeed than on the frequency of oscillation. No peaks appeared in the static airfoil or flat plate data.

Peak SPLs appear in the wake of the airfoil at the frequency of oscillation at one chord length downstream. An SPL bucket appears in some cases at two chord lengths downstream amounting to a reduction in level of 15 to 18 db. This bucket largely disappears at three chord lengths downstream at which point the SPL peak is only 3 to 6 db below that at one chord length.

In general, the SPL measurement at twice the frequency of oscillation increases by 4 to 9 db between one and two chord lengths downstream; then decreases by 4 to 7 db between two and three chord lengths. One anomalous behavior was recorded however.

The width of the airfoil wake as determined from the SPL data is more narrow for the no oscillation case than for the oscillation case with the airfoil set at the mean angle of attack used in these tests. With

oscillation and at 25 ft/sec, the wake width decreases with increasing frequency while at 100 ft/sec, it increases. There may be a Reynolds number effect on this observation.

From a comparison of the SPL spectrum data with that of the sound-level meter, it is concluded that most of the sound intensity is contained within the first and second peaks and no appreciable peaks occur at the higher harmonics.

It is concluded that within the wake, the SPL data are largely pseudosound while at one chord length above the wake, it is largely true vortex sound.

Although the SPL data have a greater dependence on airspeed than on frequency of oscillation, frequency dependent maximum values were measured at constant airspeeds above 50 ft/sec. For the airfoil, the maximum value at the fundamental frequency occurred near 28 Hz while for the first harmonic peak, it was near 20 Hz.

There does not appear to be an obvious dependency of the fundamental and first harmonic SPL peaks on reduced frequency.

From the limited amount of data, it appears that the flat plate may not be a good model for calculating the wake characteristics of a thick airfoil. This may depend upon the flat plate trailing edge configuration however.

REFERENCES

1. Blokhintsev, D. I.: Acoustics of a Nonhomogeneous Moving Medium. NACA TM 1399, 1956.

2. Jacobs, E. N.; and Sherman, A.: Airfoil Section Characteristics as Affected by Variations of the Reynolds Number. NACA TR 586, 1937.

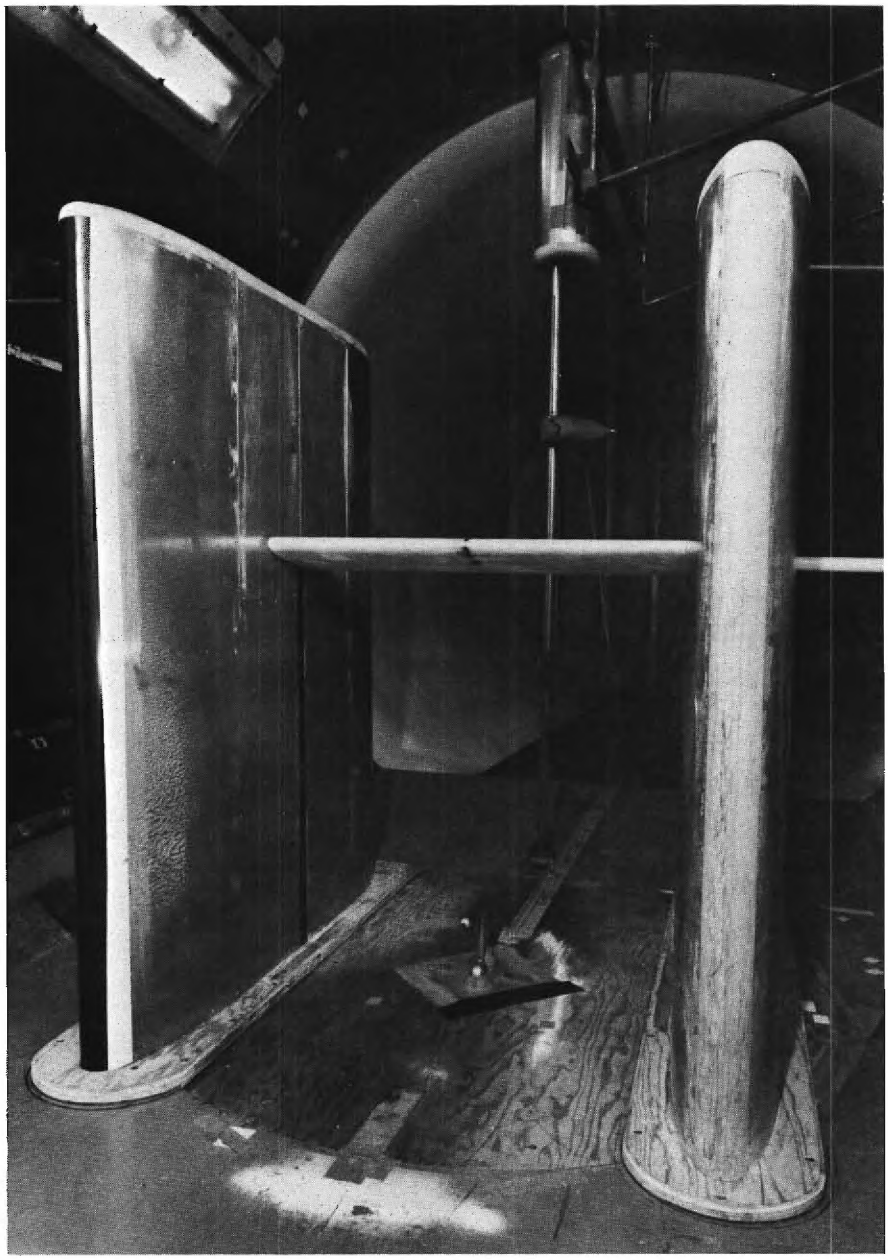

(a) Downstream View.

Figure 1. Wind Tunnel Installation of Oscillating Airfoil.

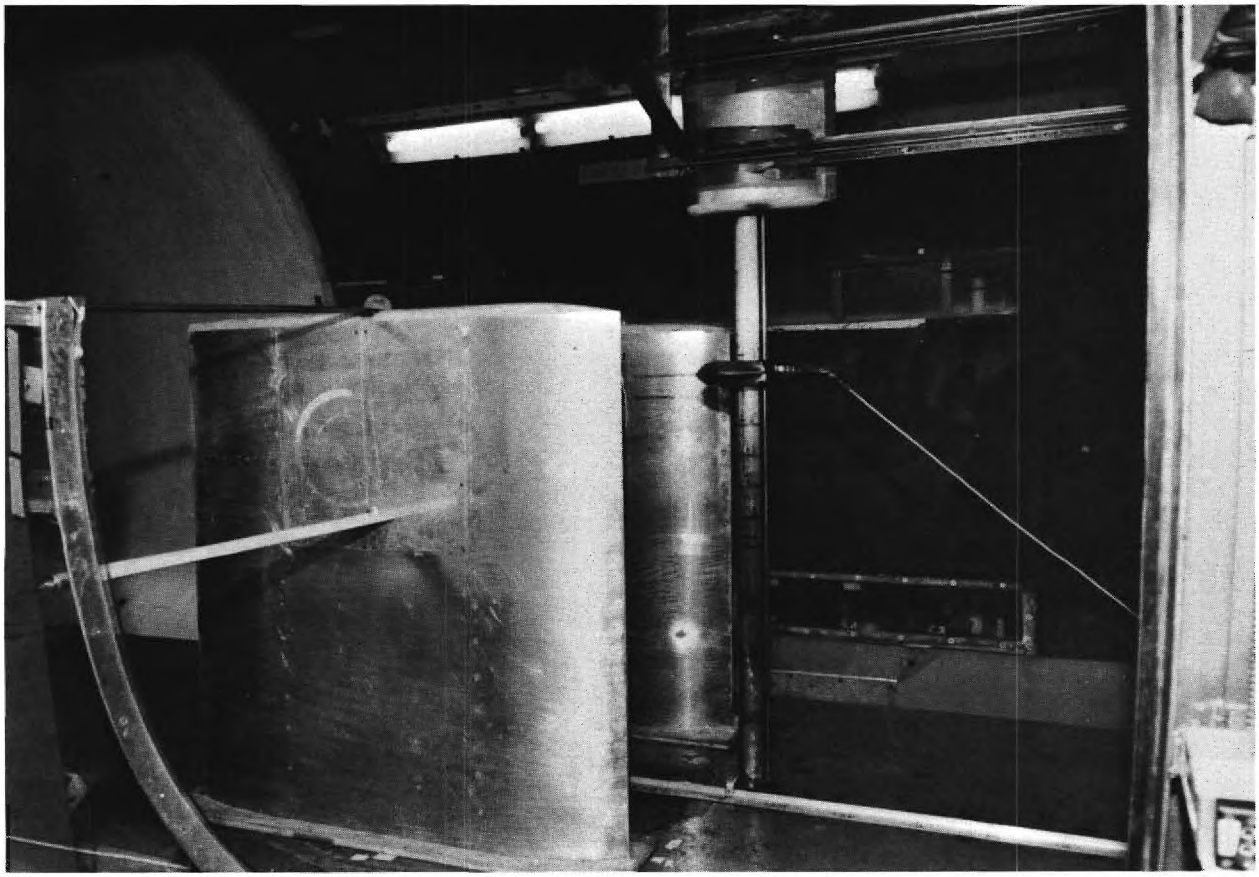

(b) Side View.

Figure 1. Concluded.

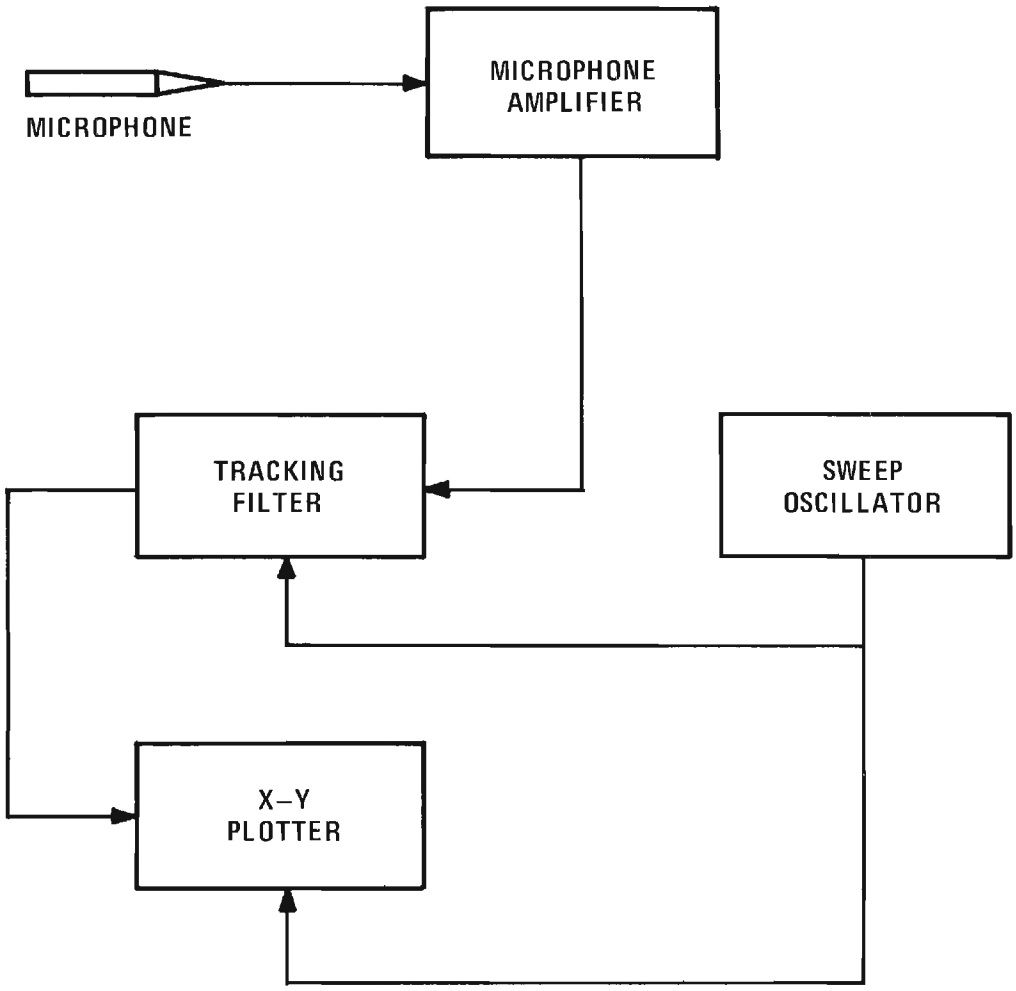

Figure 2. Flow Chart of Acoustic Measurement and Data Reduction.

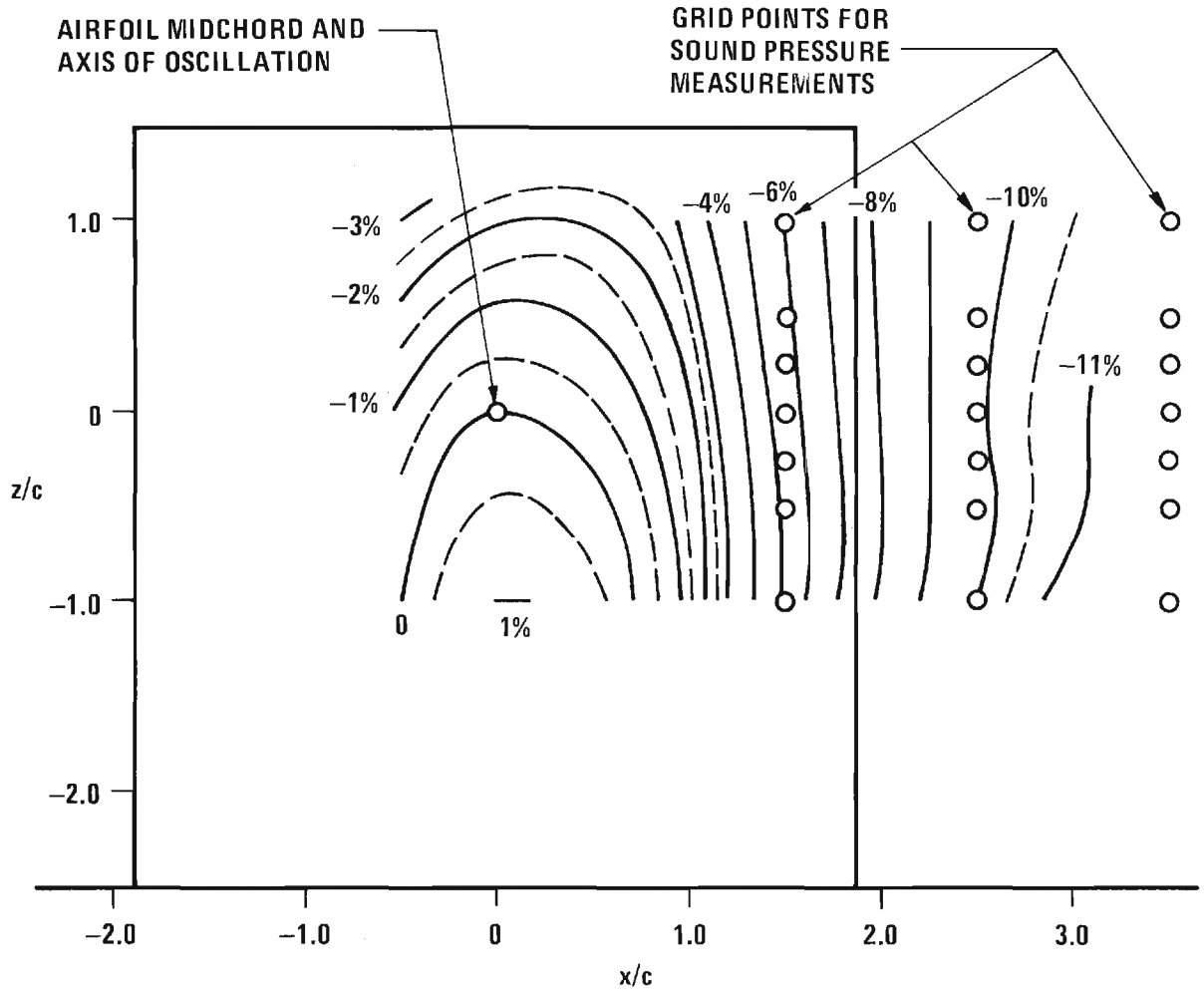

Figure 3. Lines of Constant Velocity Difference from Velocity at Airfoil Midchord Position in Longitudinal Center-line Plane with Airfoil Removed. V = 150 Ft/Sec (Typical)

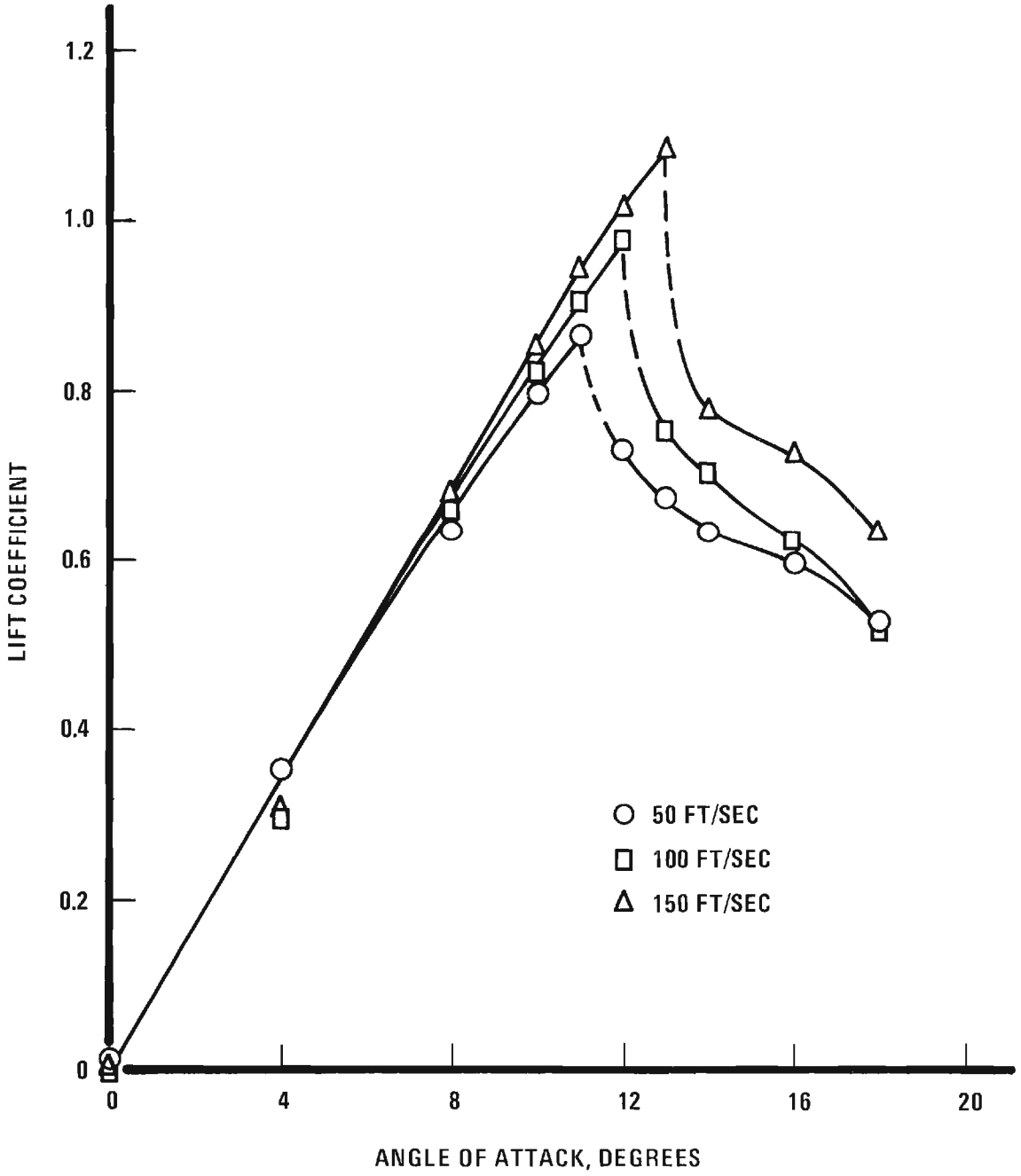

Figure 4. NACA 0012 Airfoil Lift Coefficient

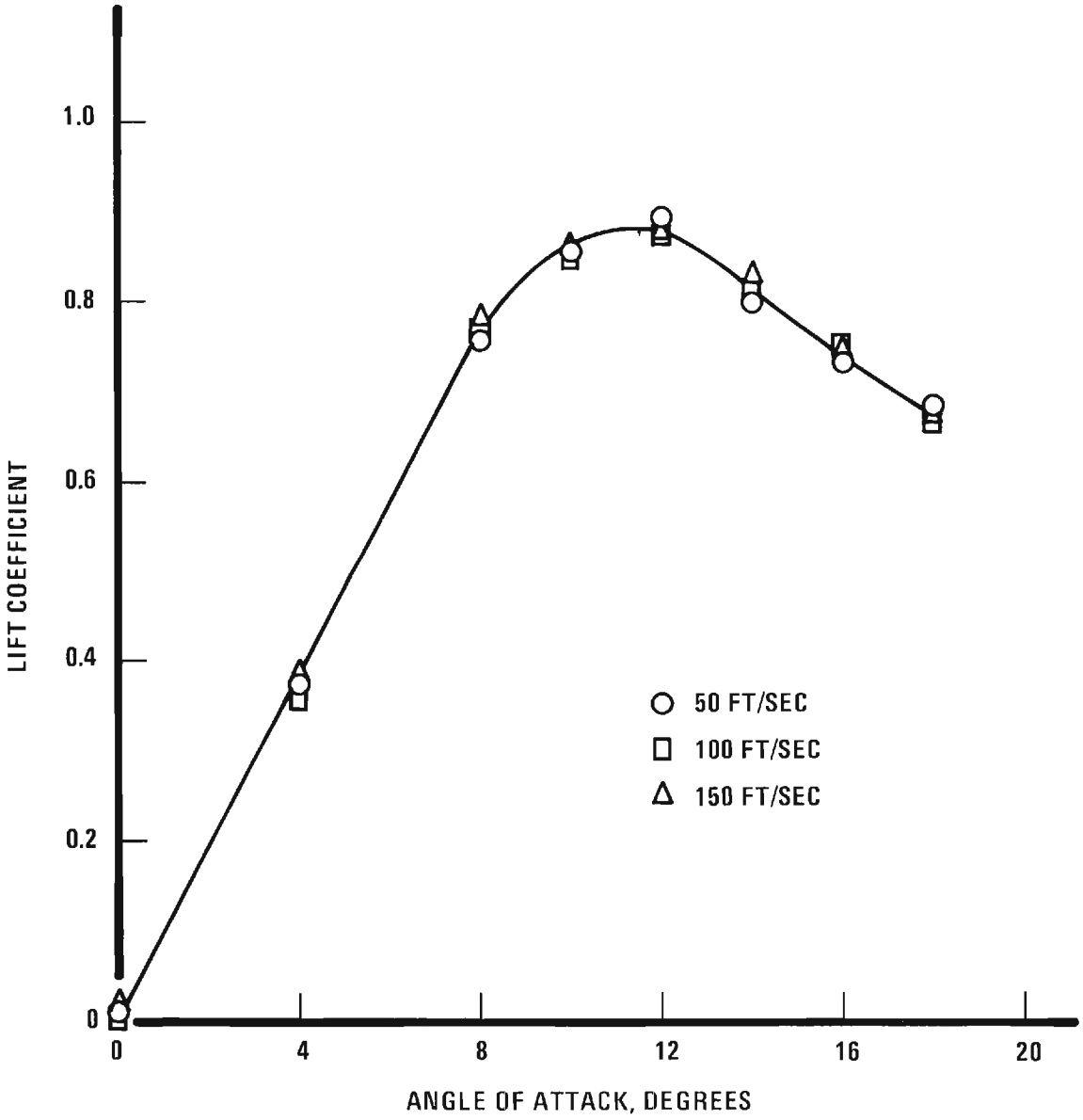

Figure 5. Flat Plate Lift Coefficient

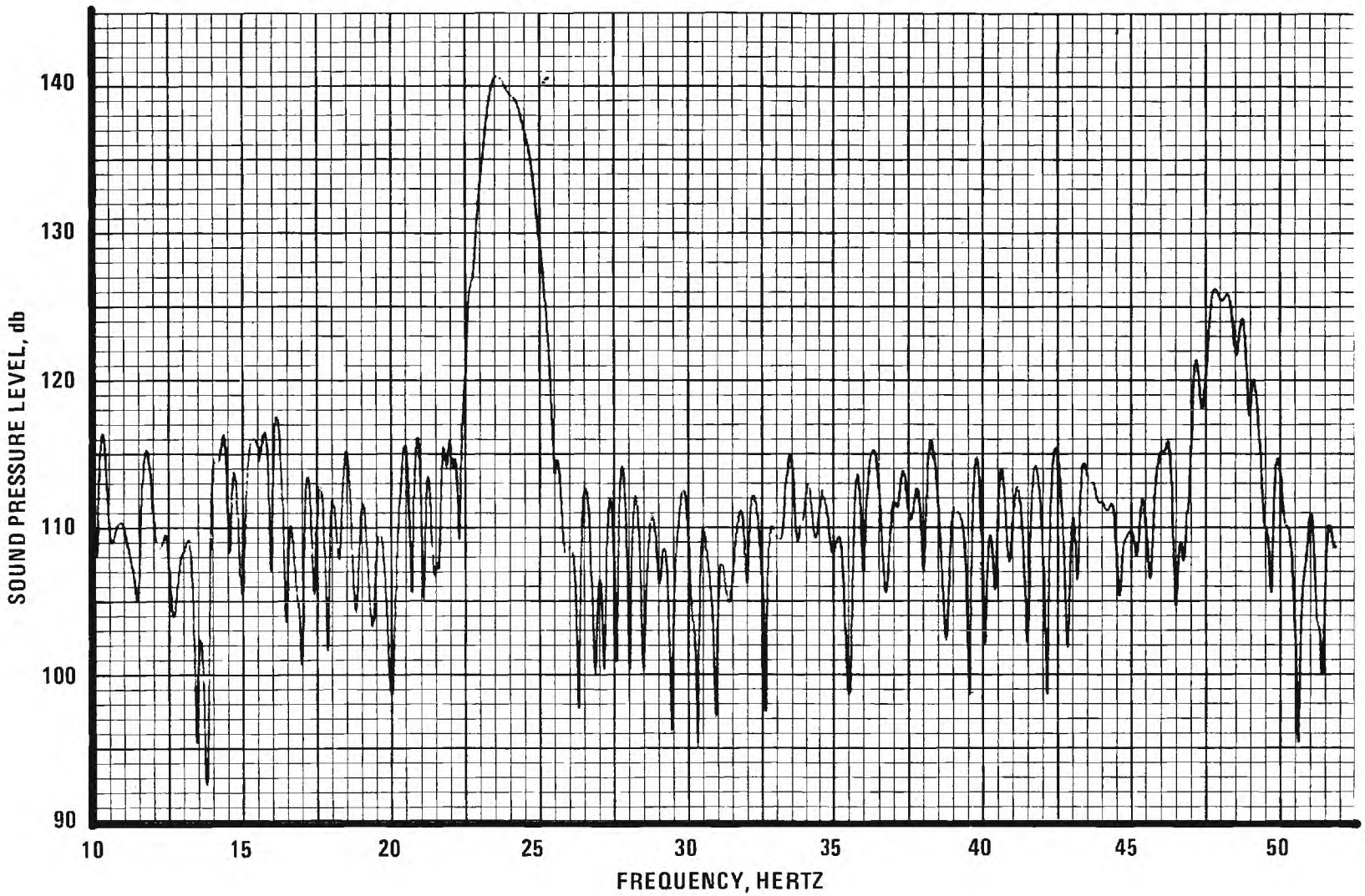

Figure 6. Sound Pressure Level in the Wake of an NACA 0012 Airfoil Oscillating at 24 Hz and Airspeed of 100 FPS

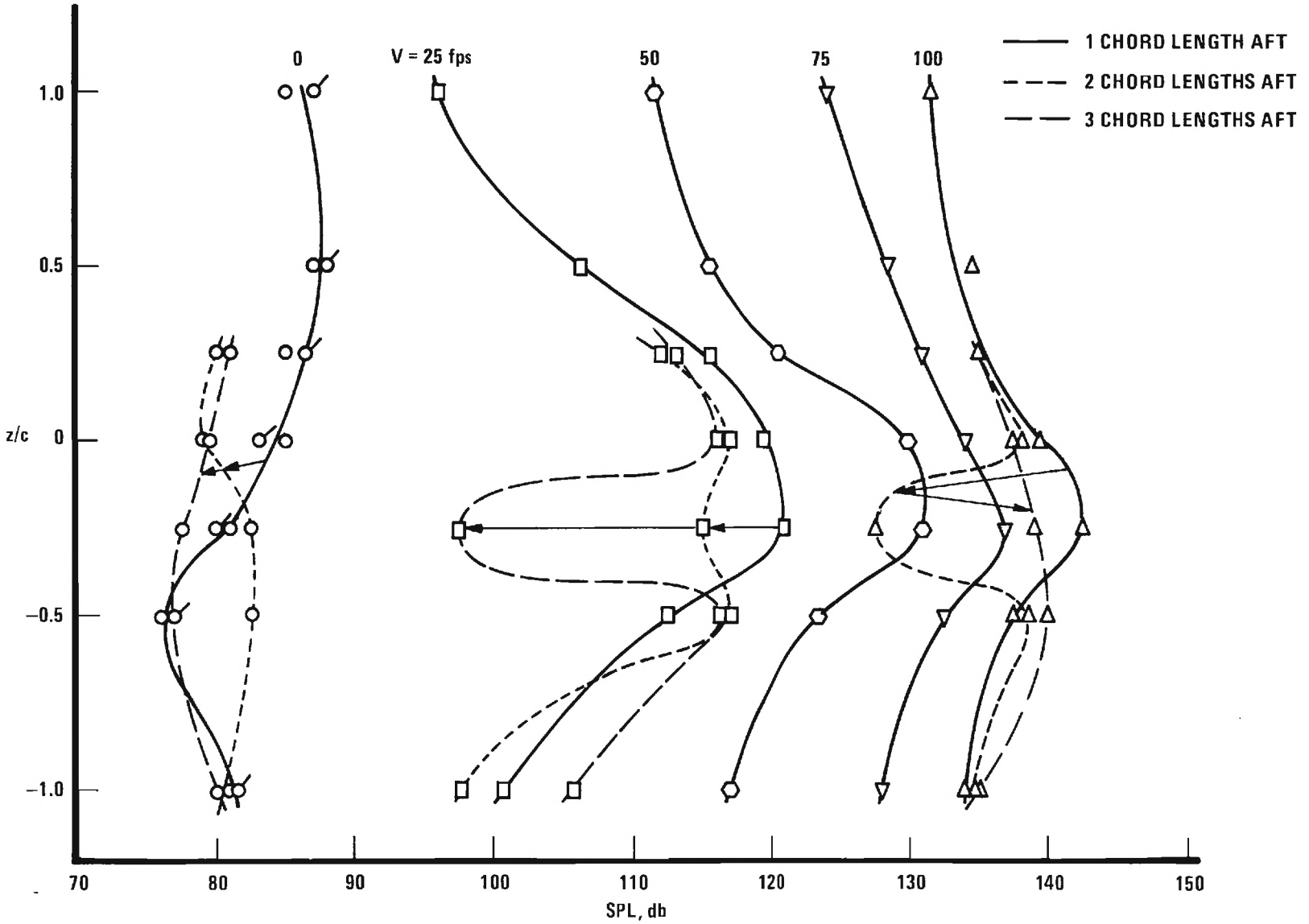

Figure 7. Variation of peak sound pressure level at the fundamental frequency in the vertical centerline plane at three positions aft of the trailing edge of an oscillating, two-dimensional NACA 0012 airfoil. f = 16 Hz.; $\alpha = 12^{\circ}$; $\Delta\alpha = \pm 3^{\circ}$.

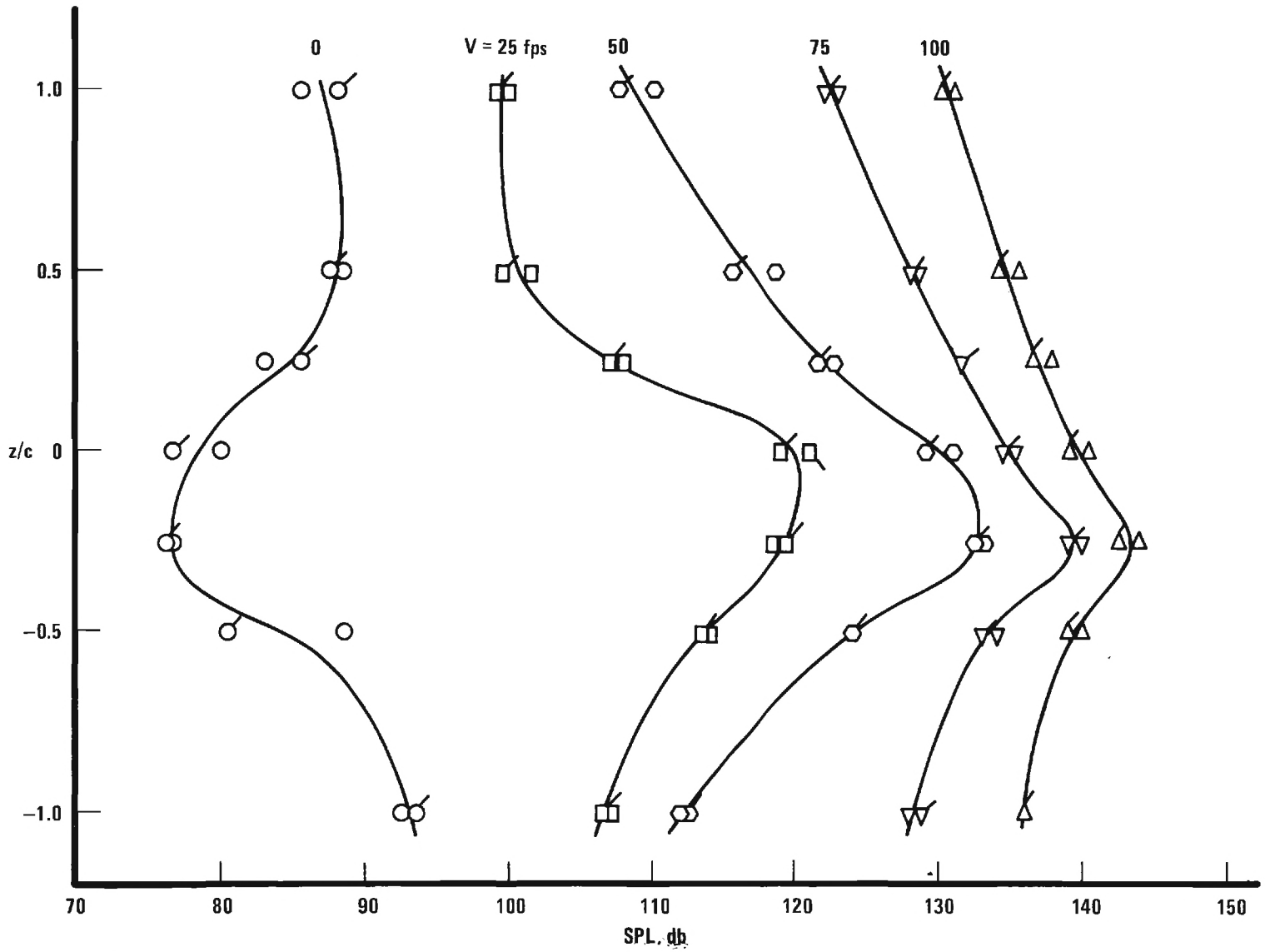

Figure 8. Variation of peak sound pressure level at the fundamental frequency in the vertical centerline plane at one chord length aft of the trailing edge of an oscillating, two-dimensional NACA 0012 airfoil. f = 20 Hz.; $\alpha = 12^{\circ}$; $\Delta\alpha = \pm 3^{\circ}$.

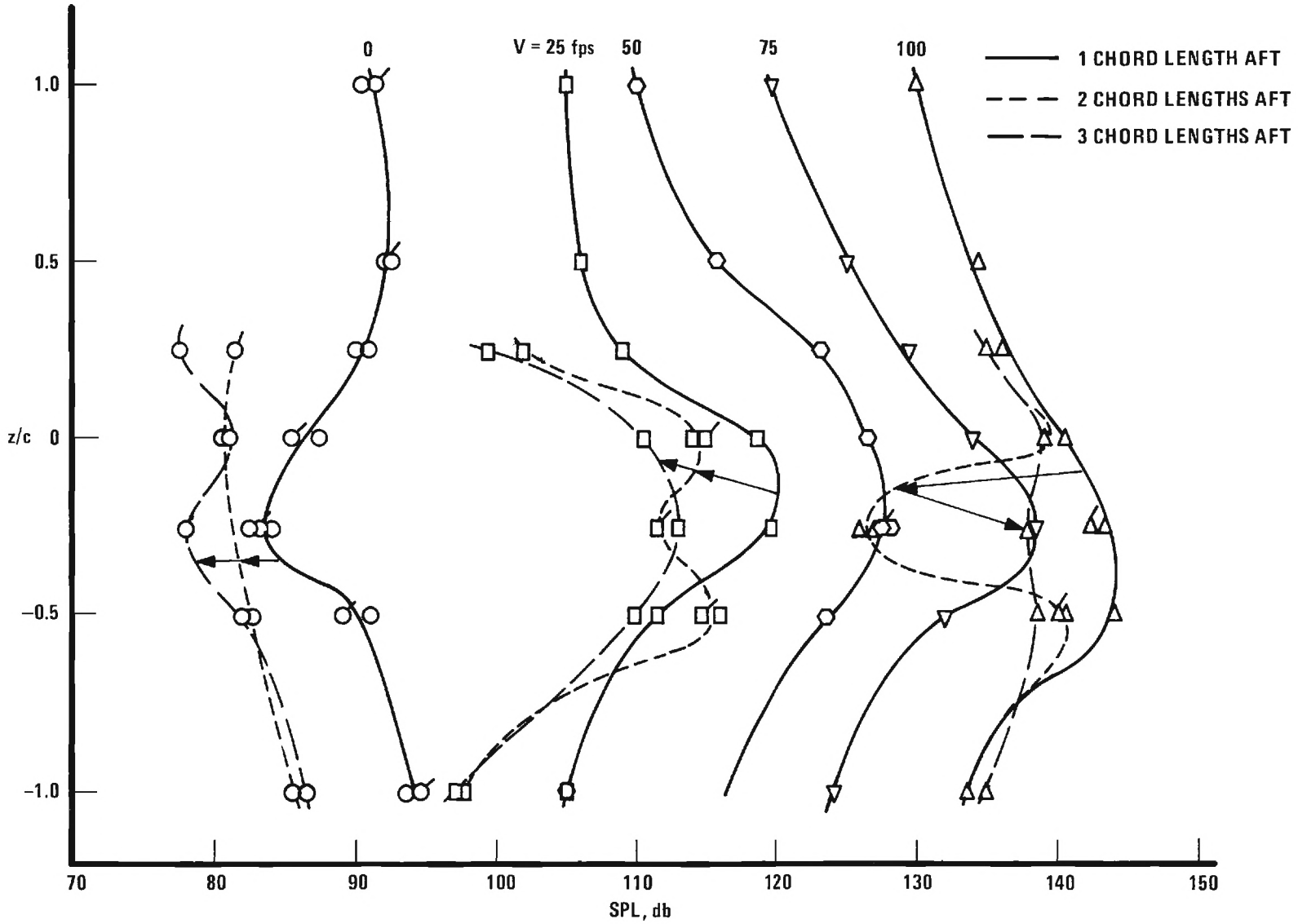

Figure 9. Variation of peak sound pressure level at the fundamental frequency in the vertical centerline plane at three positions aft of the trailing edge of an oscillating, two-dimensional NACA 0012 airfoil. f = 24 Hz.; $\alpha = 12^{\circ}$; $\Delta\alpha = \pm 3^{\circ}$.

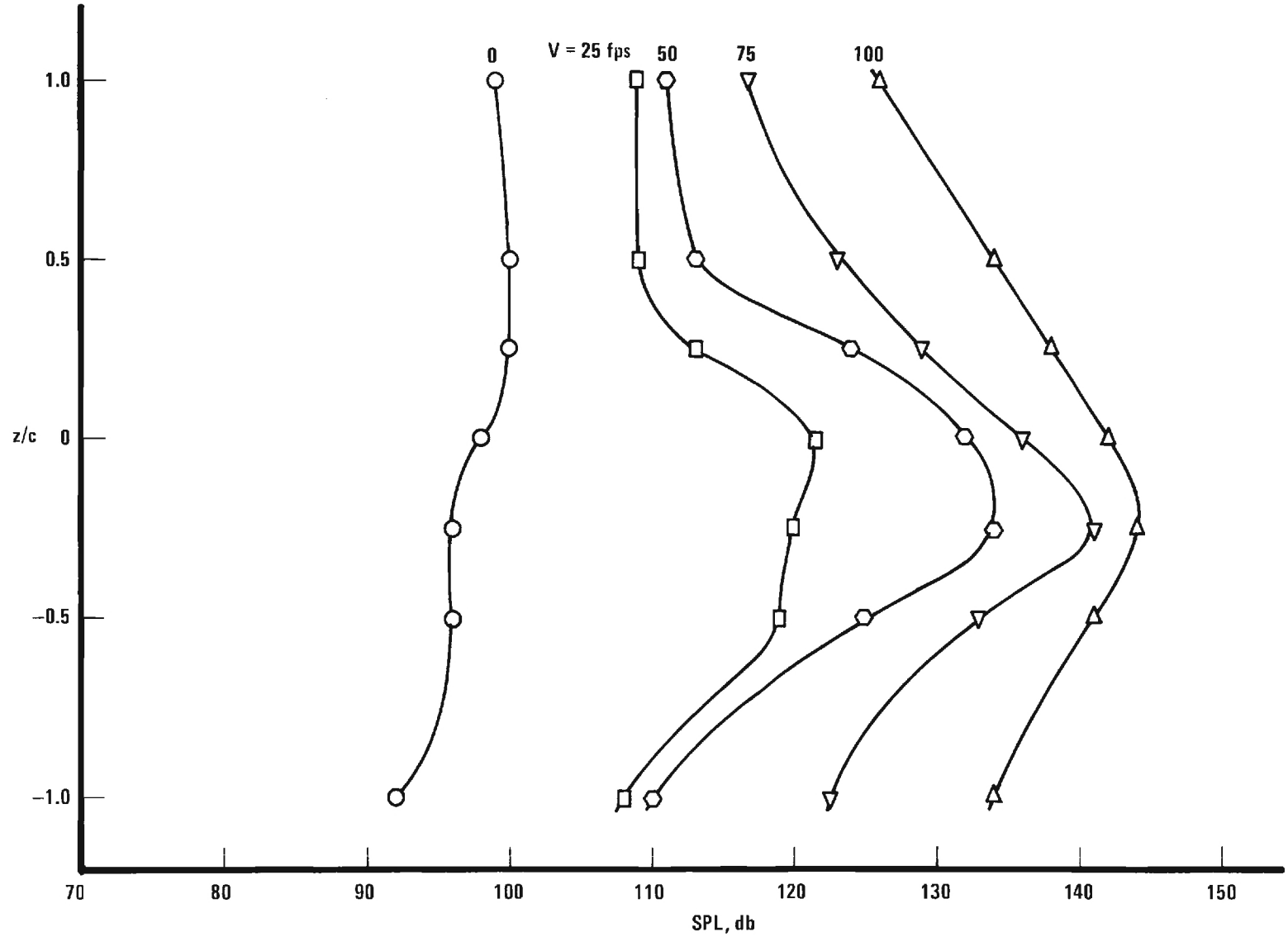

Figure 10. Variation of peak sound pressure level at the fundamental frequency in the vertical centerline plane at one chord length aft of the trailing edge of an oscillating, two-dimensional NACA 0012 airfoil. $f = 28$ Hz.; $\alpha = 12^{\circ}$; $\Delta\alpha = \pm 3^{\circ}$.

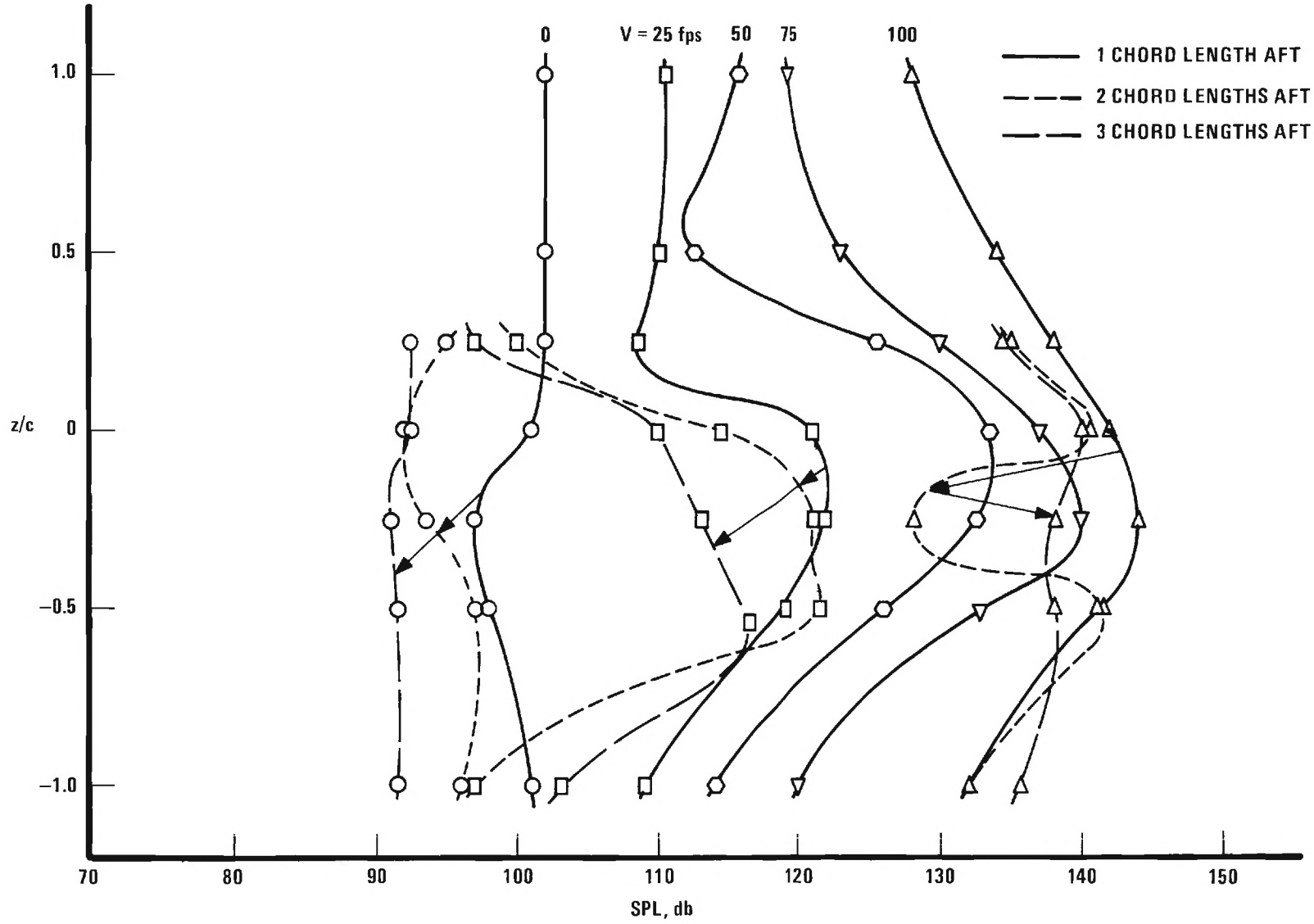

Figure 11. Variation of peak sound pressure level at the fundamental frequency in the vertical centerline plane at three positions aft of the trailing edge of an oscillating, two-dimensional NACA 0012 airfoil. f = 32 Hz.; $\alpha = 12^{\circ}$; $\Delta\alpha = \pm 3^{\circ}$.

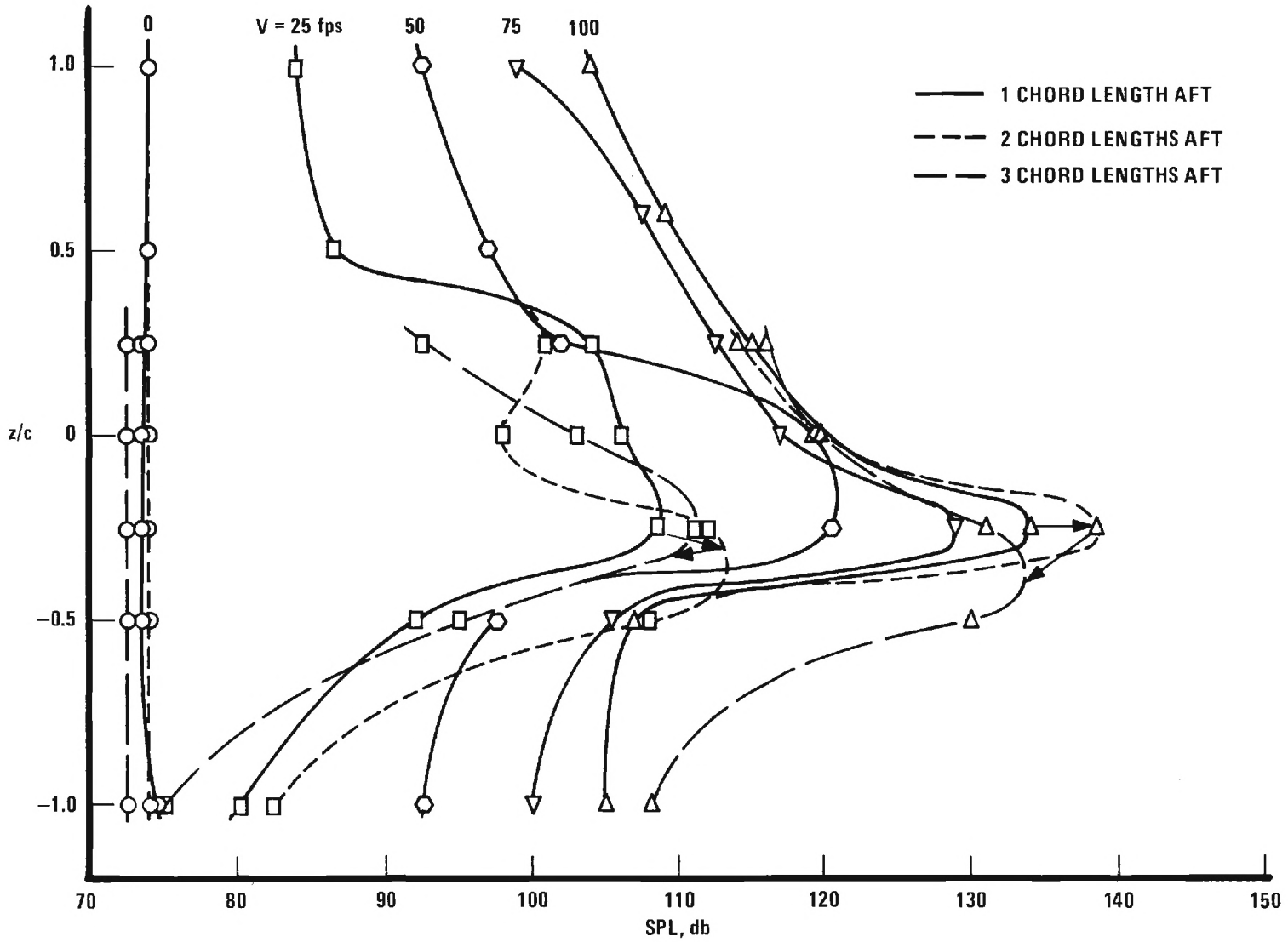

Figure 12. Variation of peak sound pressure level at first harmonic of the fundamental frequency in the vertical centerline plane at three positions aft of the trailing edge of an oscillating, two-dimensional NACA 0012 airfoil. f = 16 Hz.; $\alpha = 12^{\circ}$; $\Delta\alpha = \pm 3^{\circ}$.

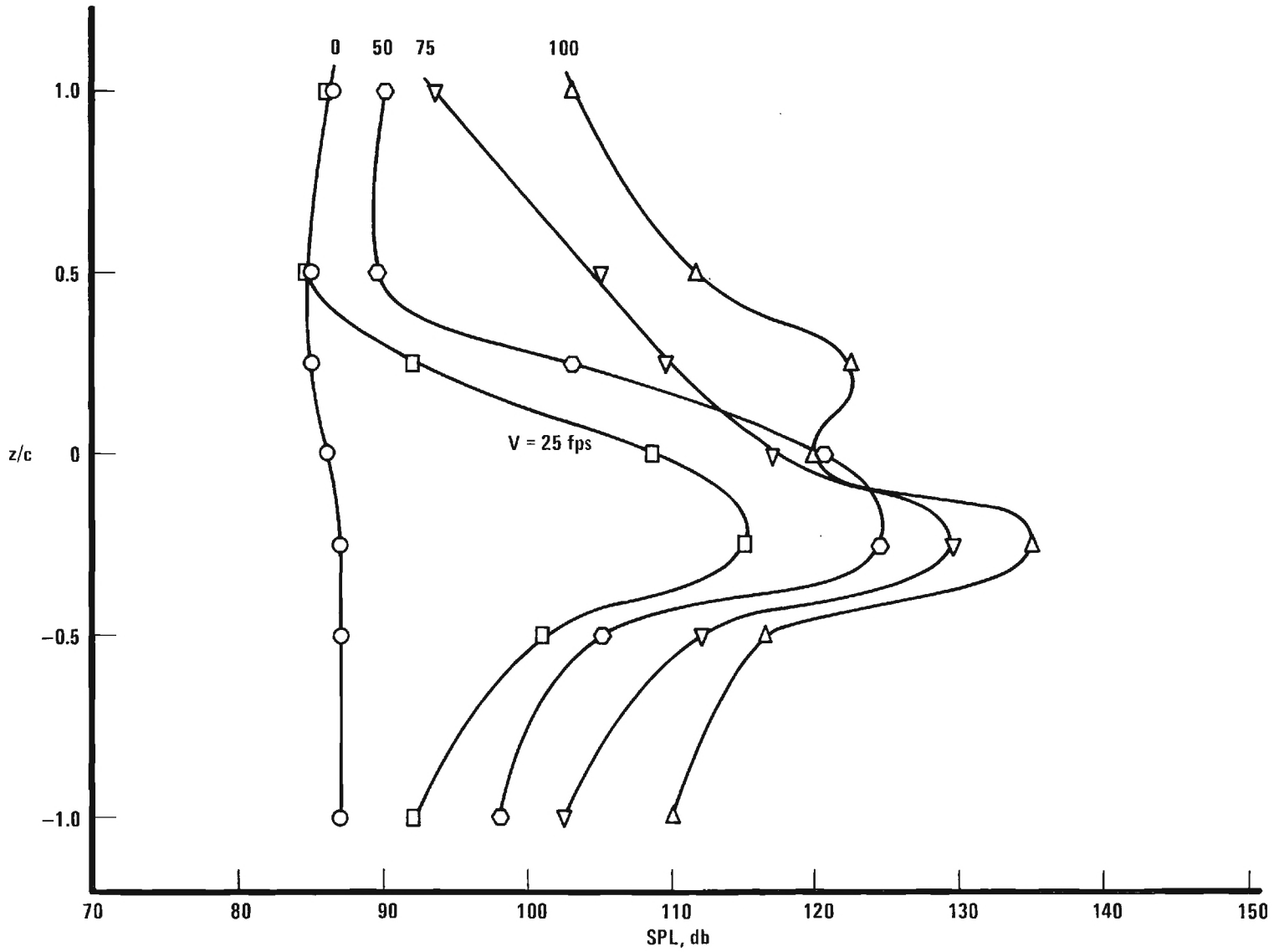

Figure 13. Variation of peak sound pressure level at first harmonic of the fundamental frequency in the vertical centerline plane at one chord length aft of the trailing edge of an oscillating, two-dimensional NACA 0012 airfoil. f = 20 Hz.; $\alpha = 12^{\circ}$; $\Delta\alpha = \pm 3^{\circ}$.

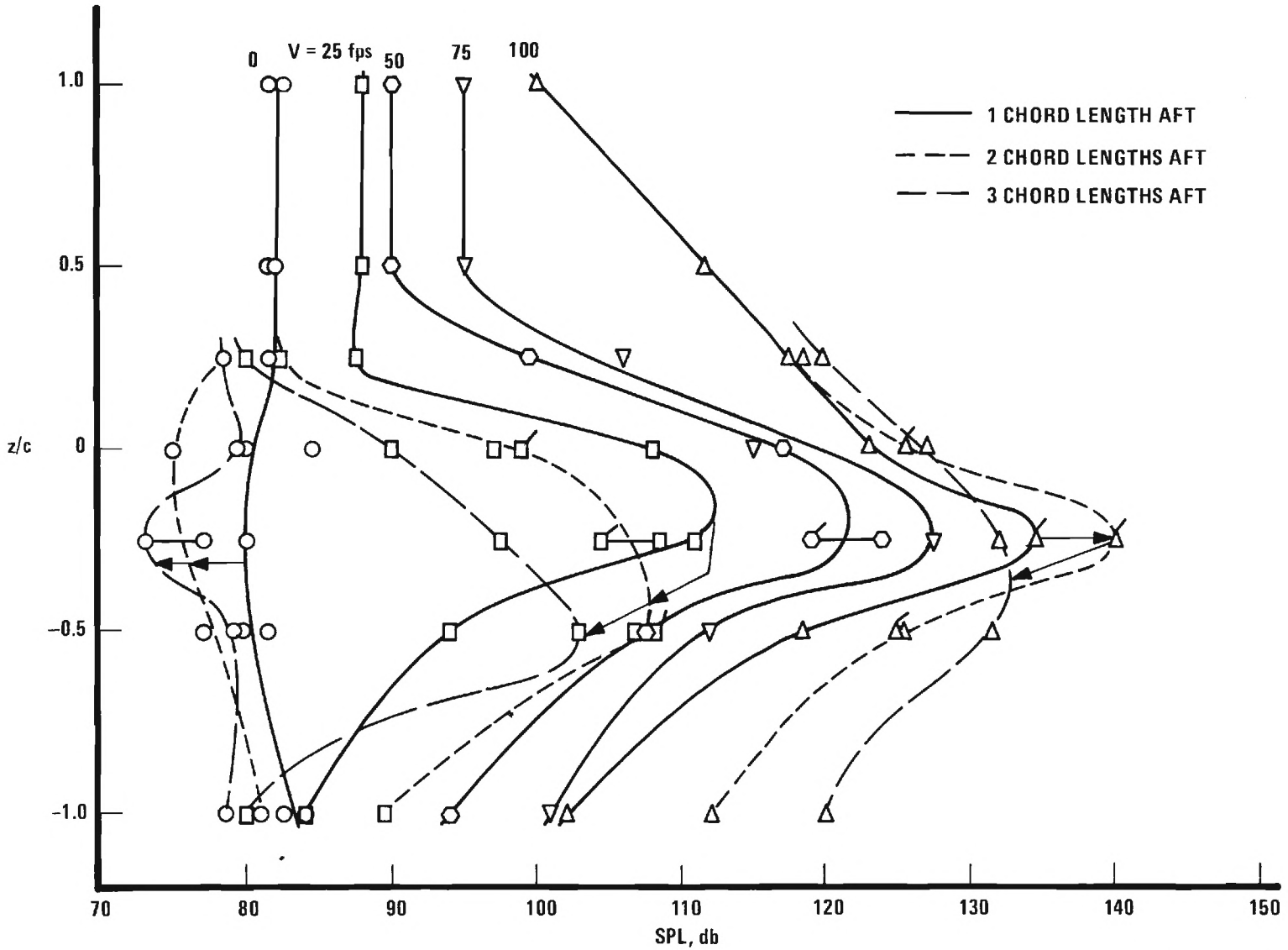

Figure 14. Variation of peak sound pressure level at first harmonic of the fundamental frequency in the vertical centerline plane at three positions aft of the trailing edge of an oscillating, two-dimensional NACA 0012 airfoil. $f = 24$ Hz.; $\alpha = 12^{\circ}$; $\Delta\alpha = \pm 3^{\circ}$.

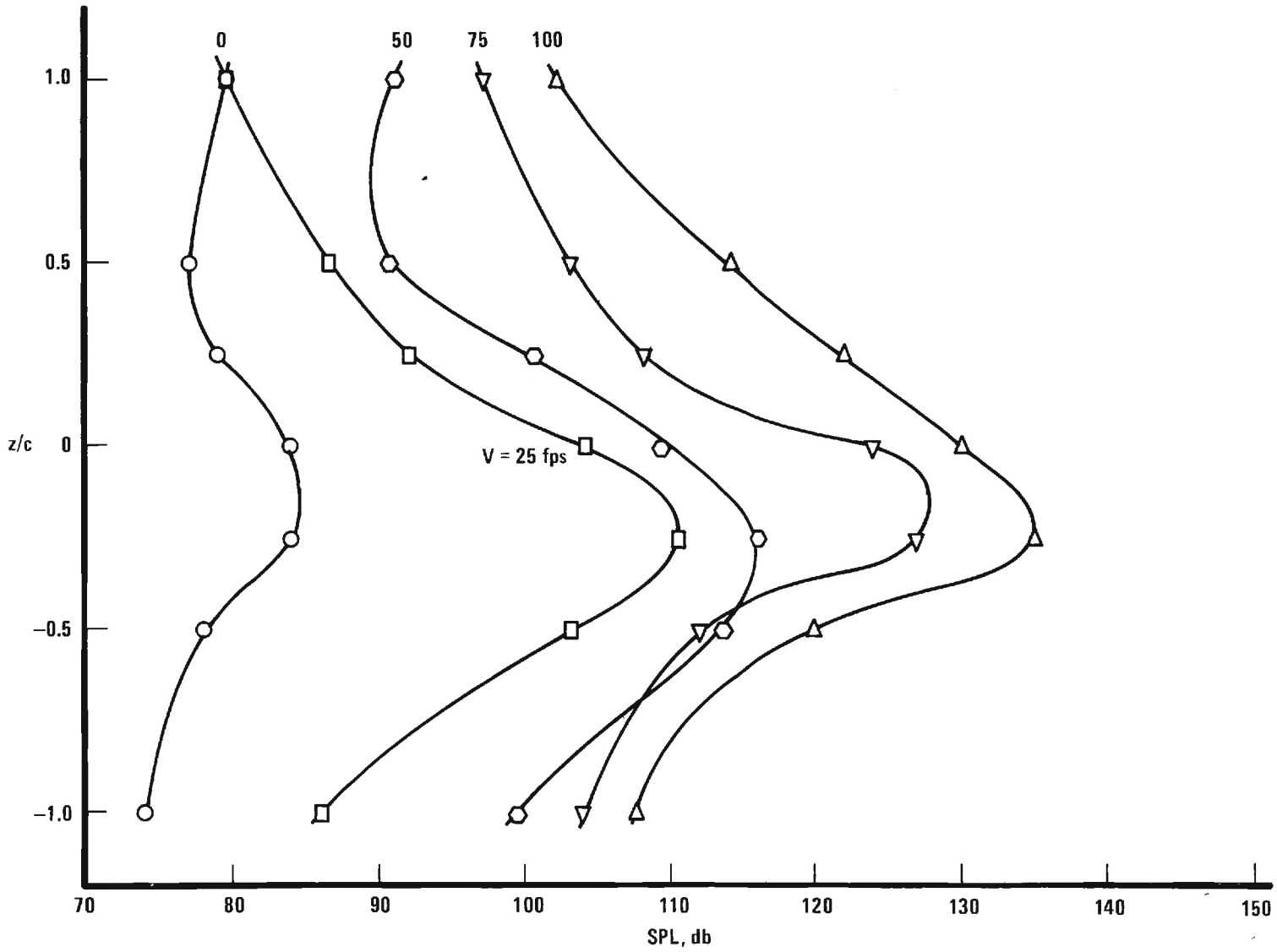

Figure 15. Variation of peak sound pressure level at first harmonic of the fundamental frequency in the vertical centerline plane at one chord length aft of the trailing edge of an oscillating, two-dimensional NACA 0012 airfoil. f = 28 Hz.; $\alpha = 12^{\circ}$; $\Delta\alpha = \pm 3^{\circ}$.

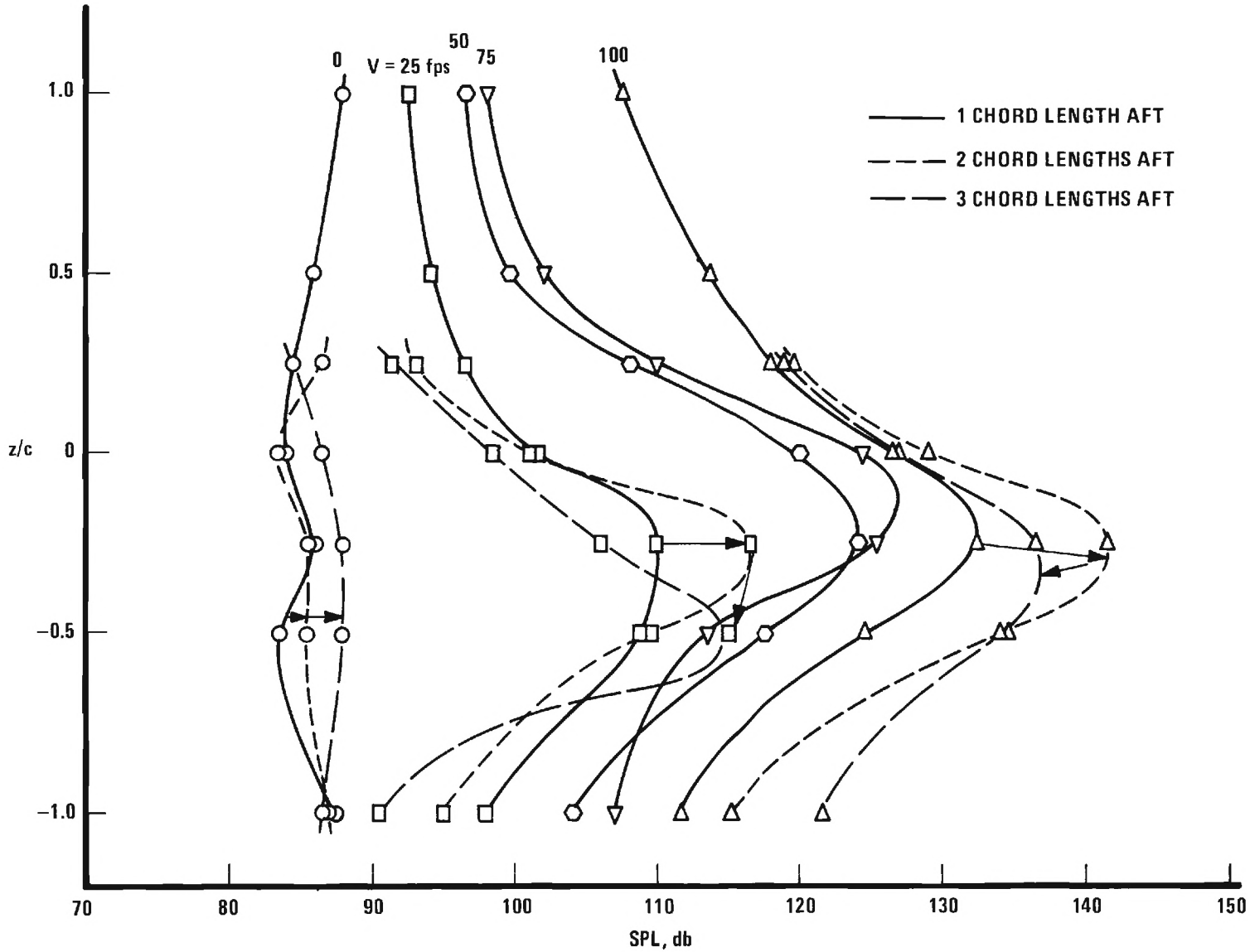

Figure 16. Variation of peak sound pressure level at first harmonic of the fundamental frequency in the vertical centerline plane at three positions aft of the trailing edge of an oscillating, two-dimensional NACA 0012 airfoil. f = 32 Hz.; $\alpha = 12^{\circ}$; $\Delta\alpha = \pm 3^{\circ}$.

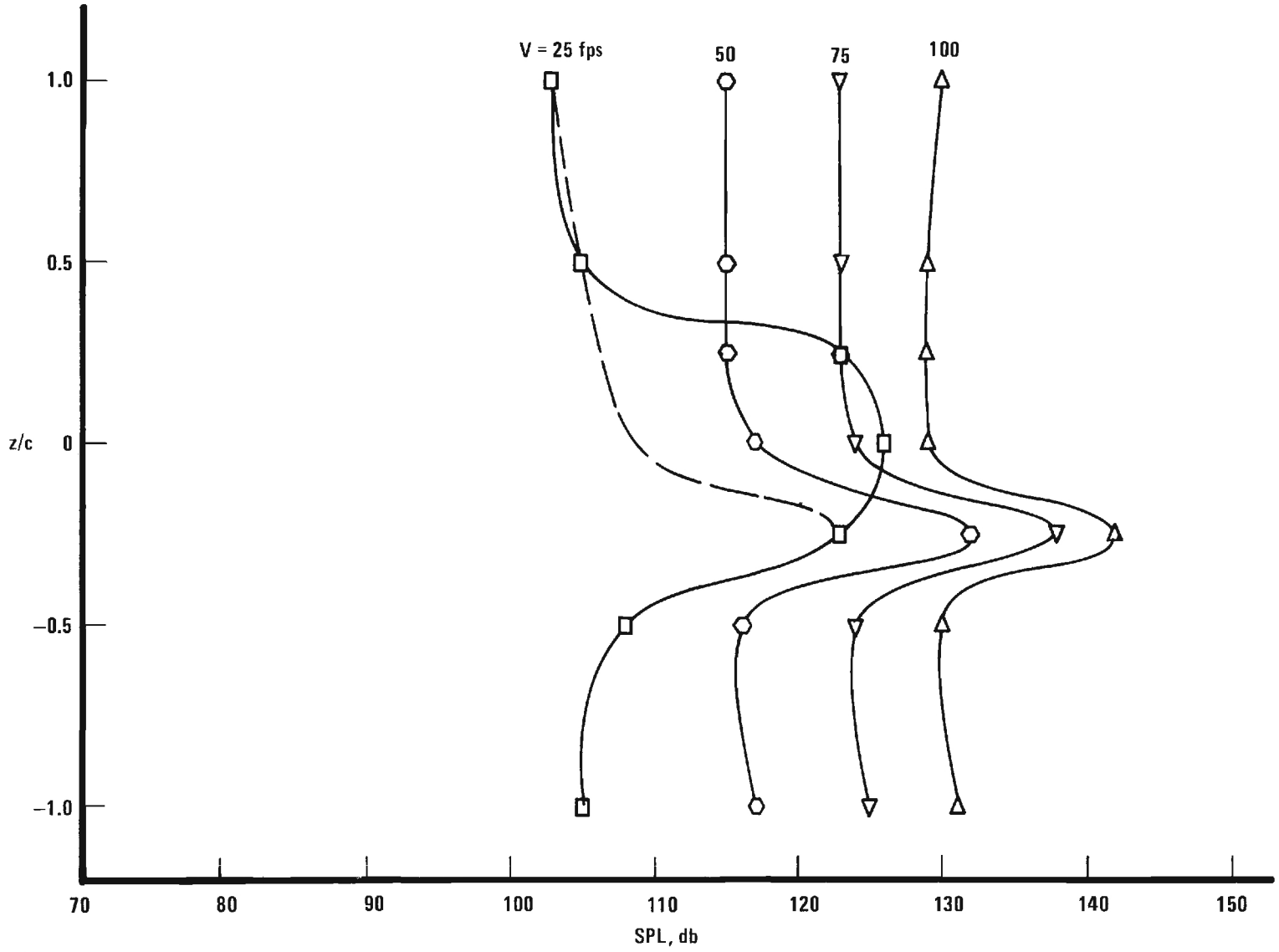

Figure 17. Variation of overall sound pressure level in the vertical centerline plane at one chord length aft of the trailing edge of a two-dimensional NACA 0012 airfoil. f = 0 Hz.; $\alpha = 12^{\circ}$.

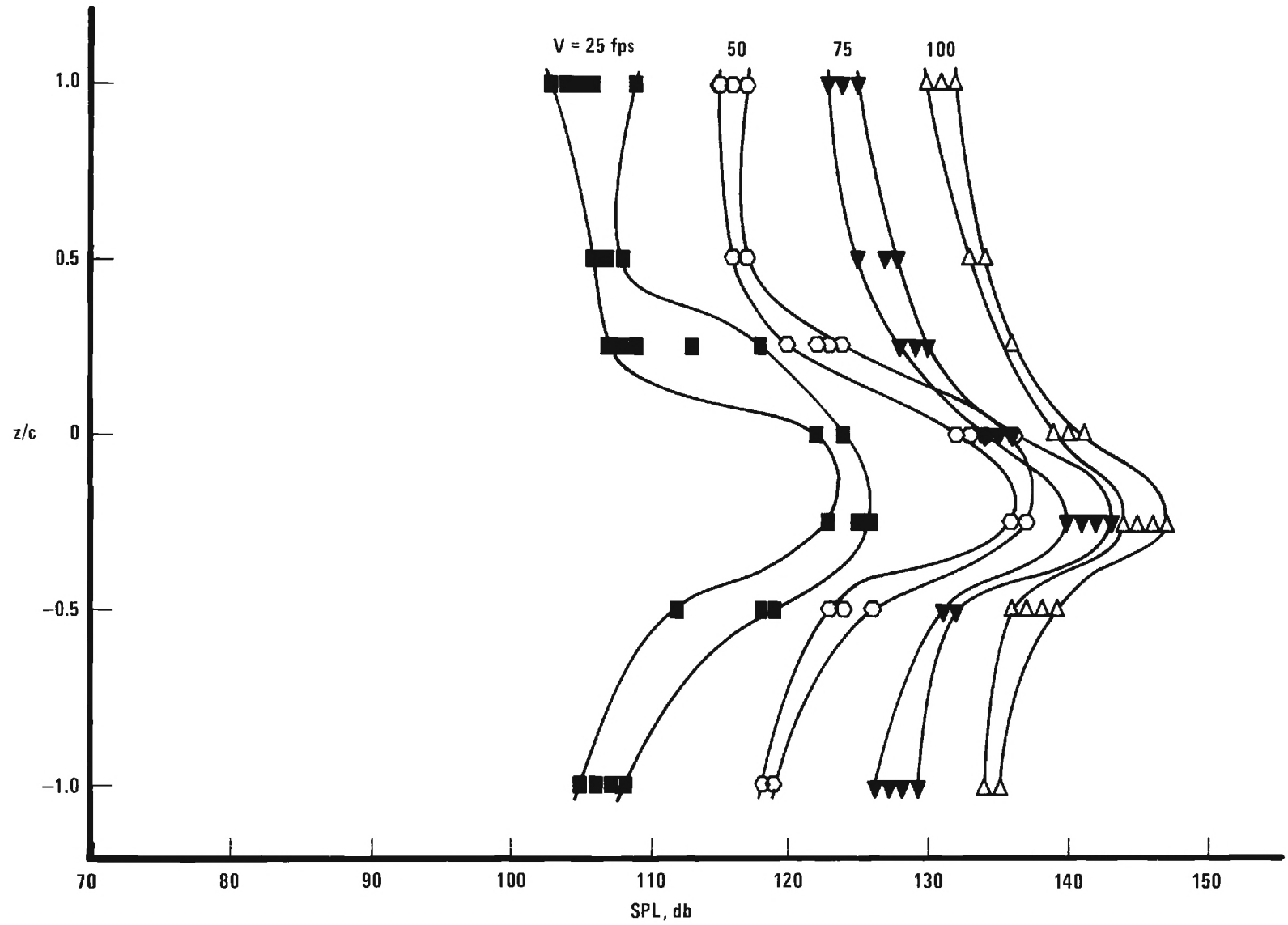

Figure 18. Variation of overall sound pressure level in the vertical centerline plane at one chord length aft of the trailing edge of an oscillating, two-dimensional NACA 0012 airfoil. f = 16, 20, 24, 28, 32 Hz.; $\alpha = 12^{\circ}$; $\Delta\alpha = \pm 3^{\circ}$.

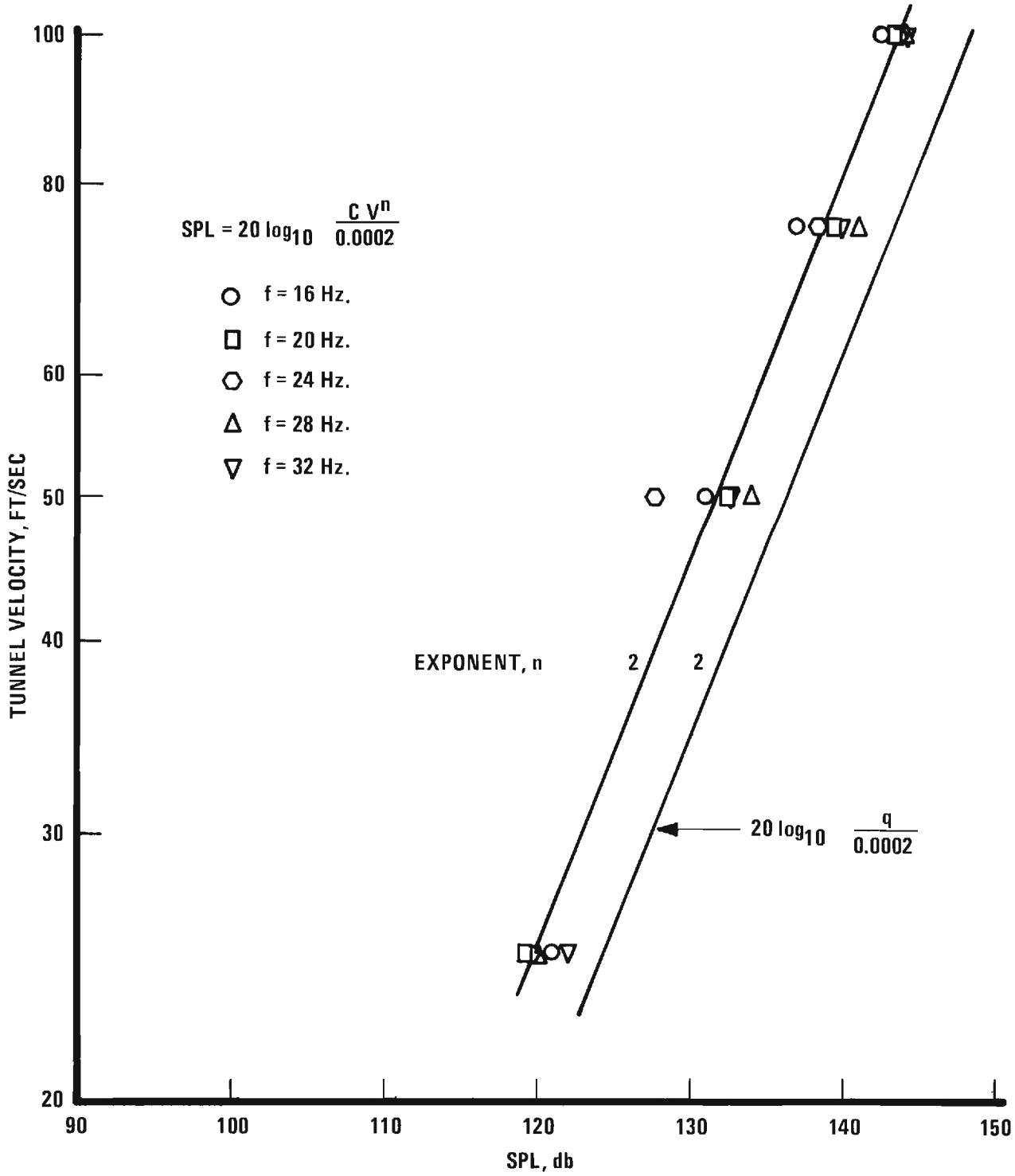

Figure 19. Peak sound pressure level at the fundamental frequency as a function of velocity behind the trailing edge of an oscillating, two-dimensional NACA airfoil. $z/c = -0.25$; $x/c = 1.0$; $\alpha = 12^{\circ}$; $\Delta\alpha = \pm 3^{\circ}$.

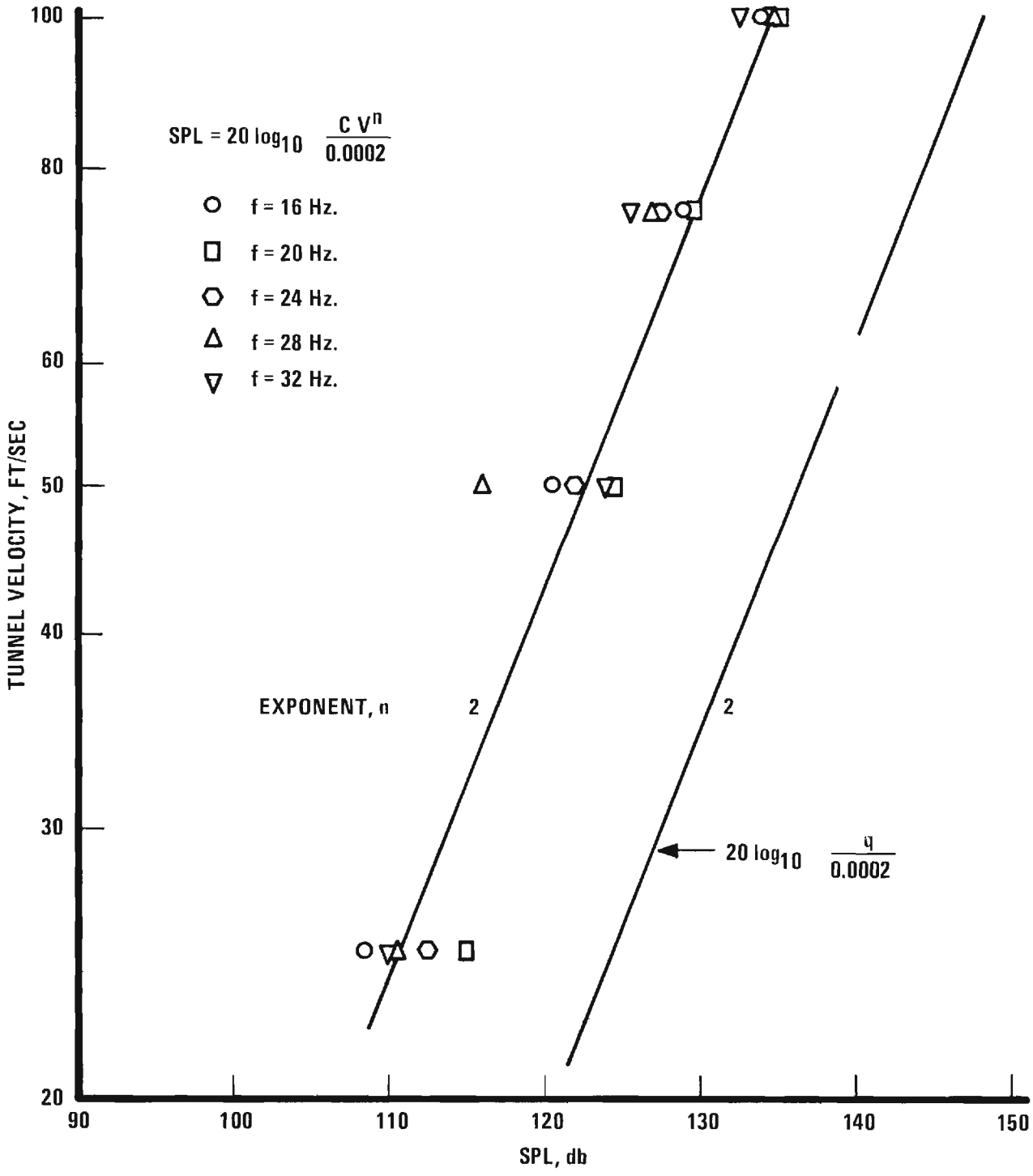

Figure 20. Peak sound pressure level at first harmonic of the fundamental frequency as a function of velocity behind the trailing edge of an oscillating, two-dimensional NACA airfoil. $z/c = -0.25$; $x/c = 1.0$; $\alpha = 12^{\circ}$; $\Delta\alpha = \pm 3^{\circ}$.

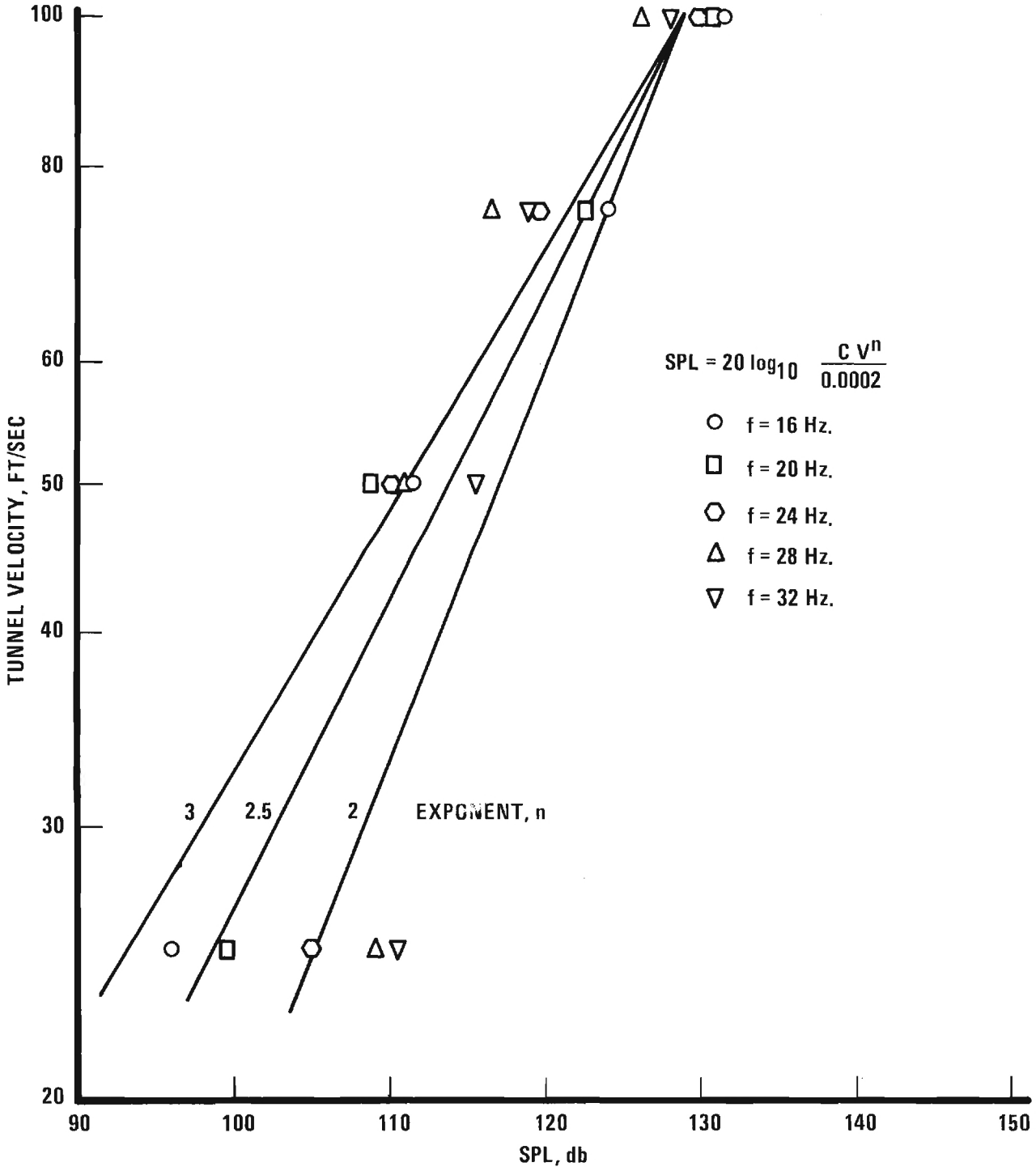

Figure 21. Peak sound pressure level at the fundamental frequency as a function of velocity behind the trailing edge of an oscillating, two-dimensional NACA 0012 airfoil. z/c = 1.0; x/c = 1.0; $\alpha = 12^{\circ}$; $\Delta\alpha = \pm 3^{\circ}$.

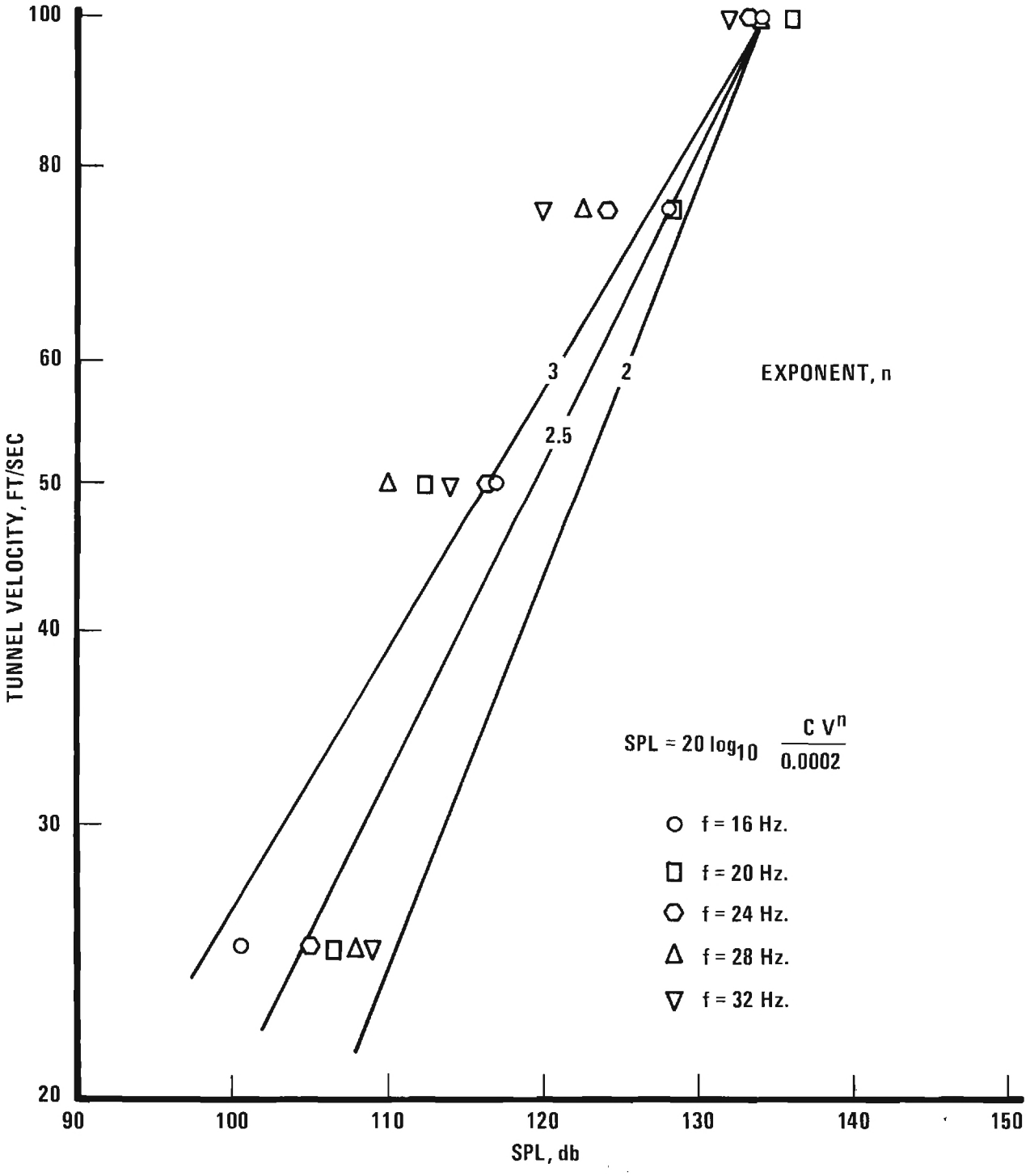

Figure 22. Peak sound pressure level at the fundamental frequency as a function of velocity behind the trailing edge of an oscillating, two-dimensional NACA 0012 airfoil. $z/c = -1.0$; $x/c = 1.0$; $\alpha = 12^{\circ}$; $\Delta\alpha = \pm 3^{\circ}$.

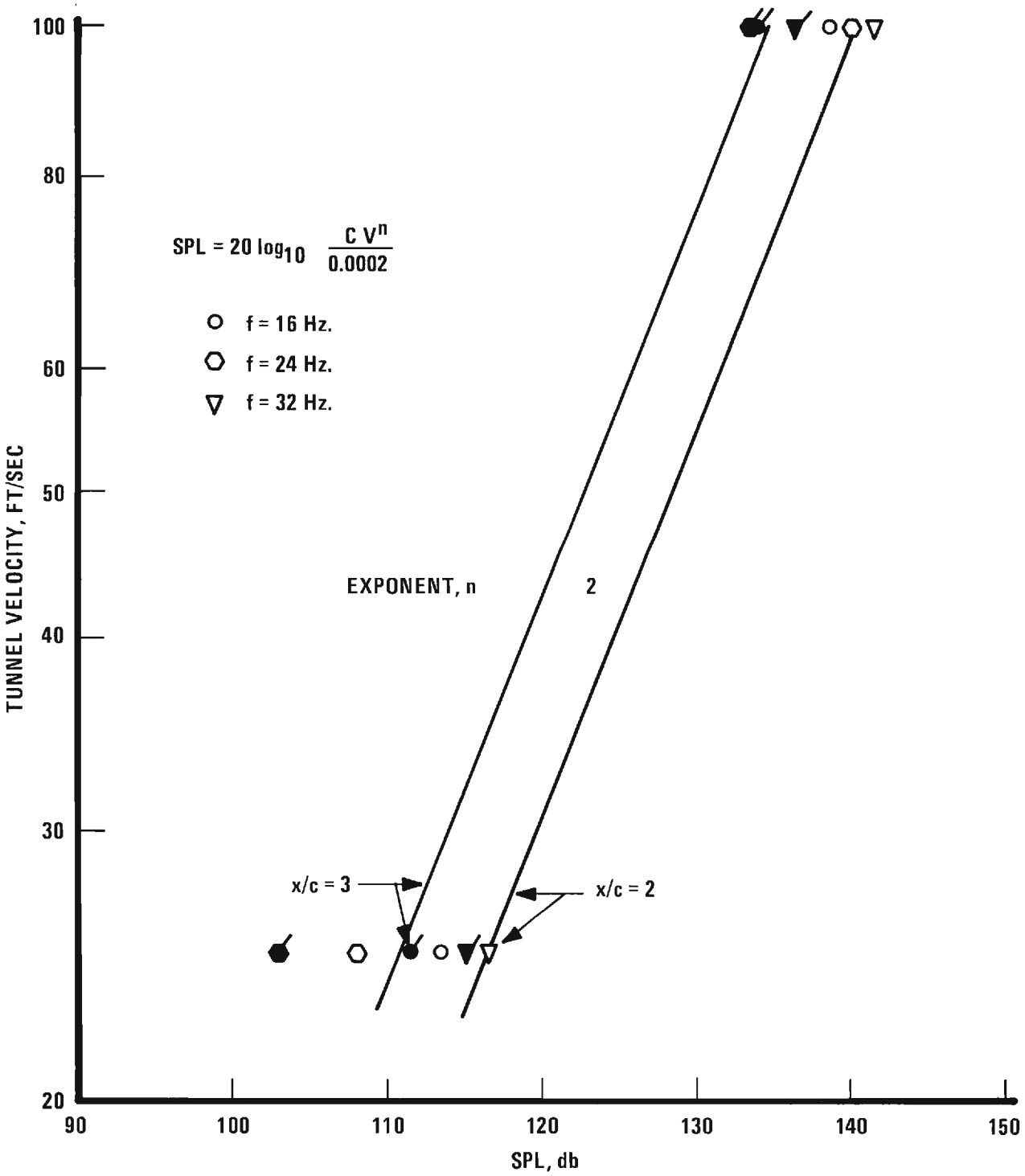

Figure 23. Peak sound pressure level at first harmonic of the fundamental frequency as a function of velocity at two streamwise positions behind the trailing edge of an oscillating, two-dimensional NACA airfoil. $z/c = -0.25$; $\alpha = 12^{\circ}$; $\Delta\alpha = \pm 3^{\circ}$.

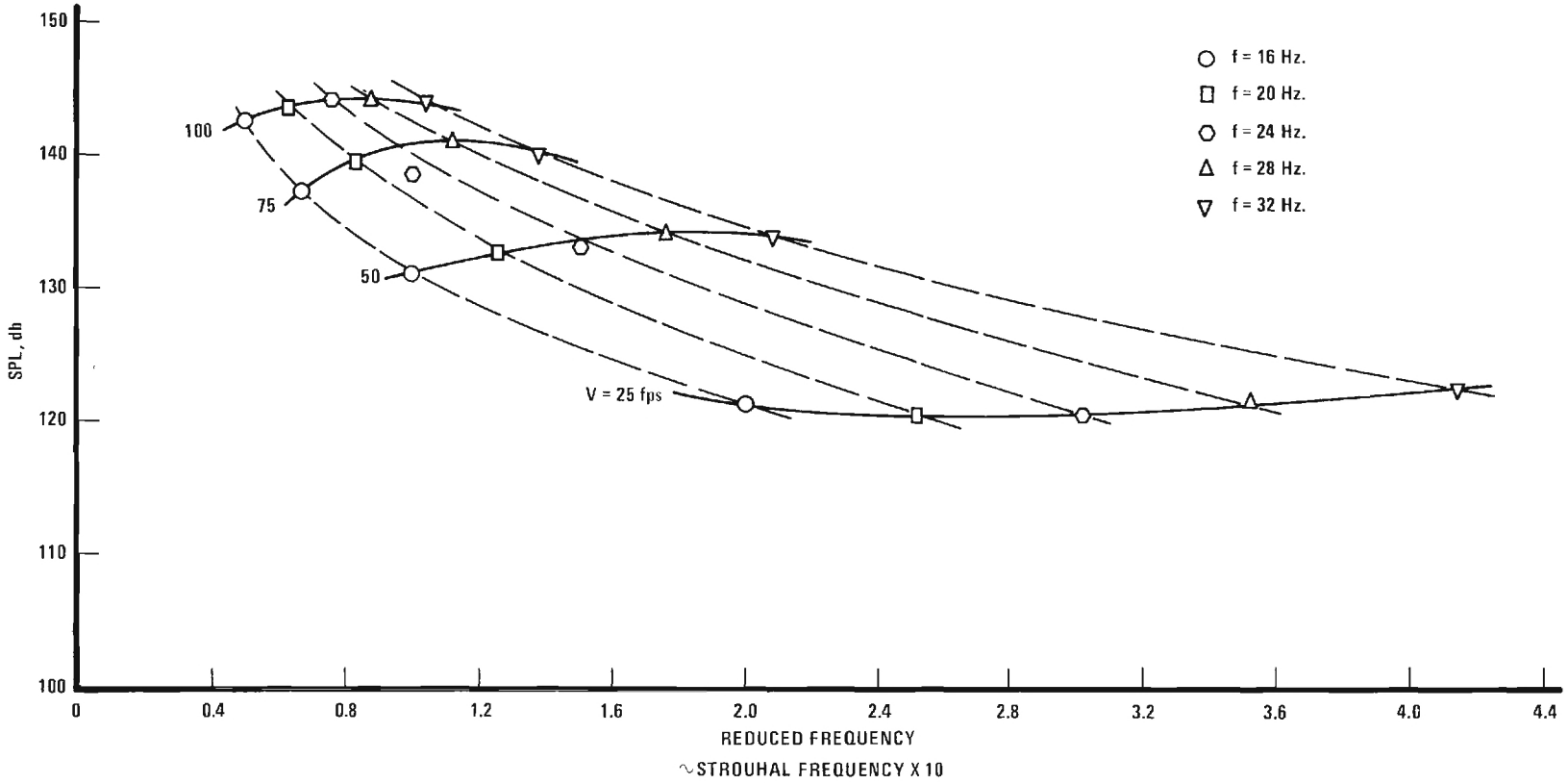

Figure 24. Peak sound pressure level at the fundamental frequency as a function of reduced frequency behind the trailing edge of an oscillating, two-dimensional NACA 0012 airfoil. $x/c = 1.0$; $\alpha = 12^{\circ}$; $\Delta\alpha = \pm 3^{\circ}$.

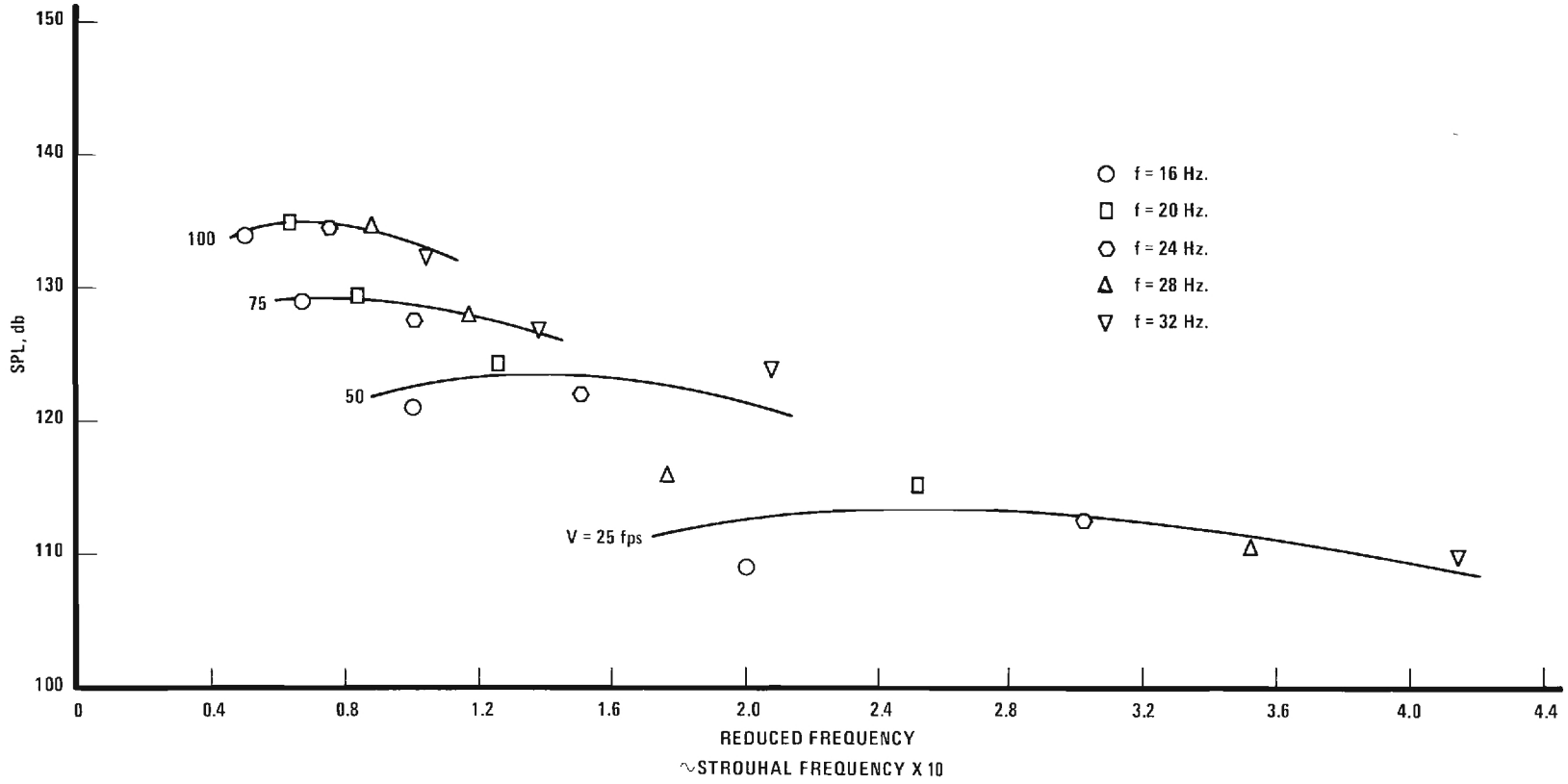

Figure 25. Peak sound pressure level at first harmonic of the fundamental frequency as a function of reduced frequency behind the trailing edge of an oscillating, two-dimensional NACA 0012 airfoil. $x/c = 1.0$; $\alpha = 12^{\circ}$; $\Delta\alpha = \pm 3^{\circ}$.

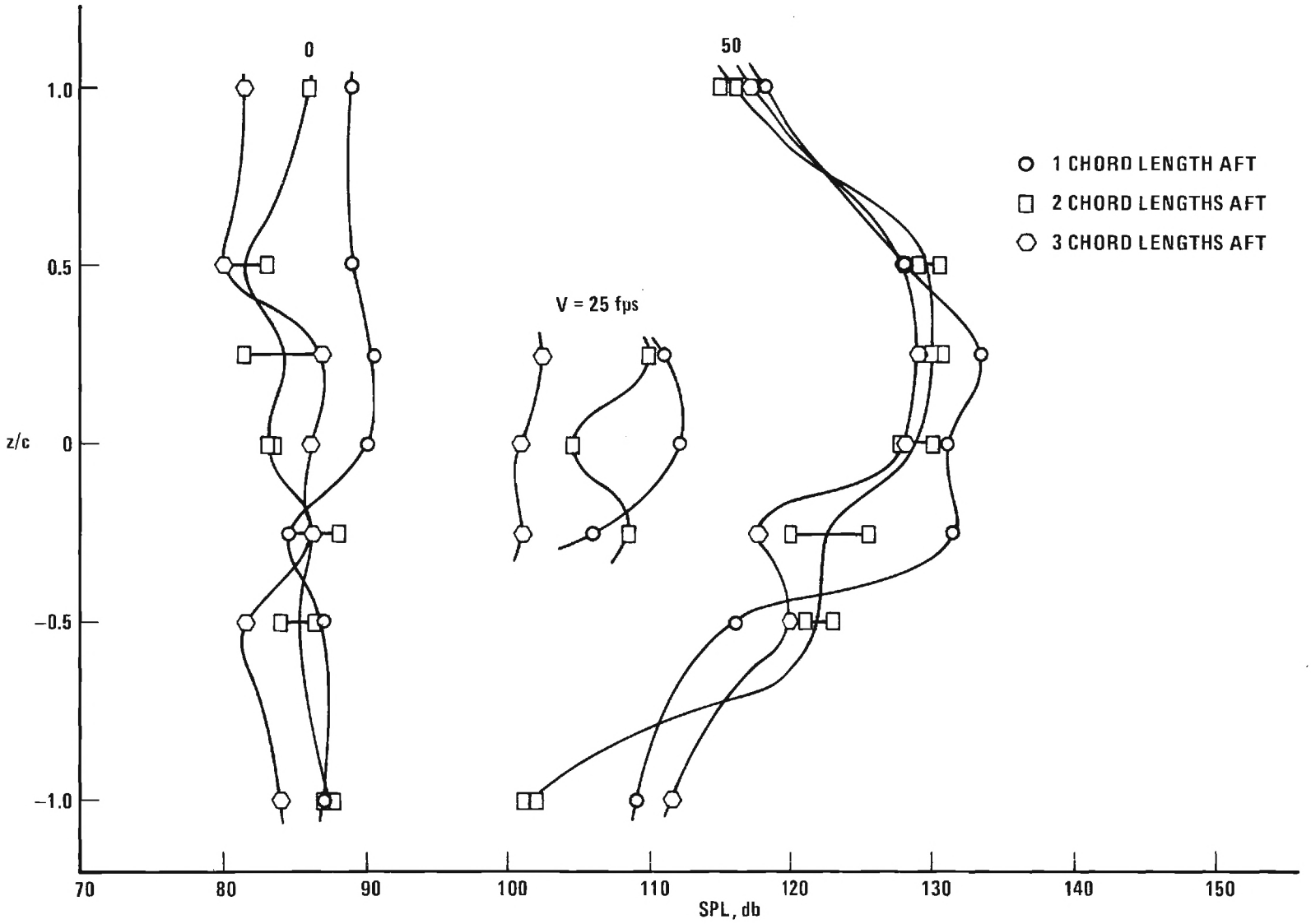

Figure 26. Variation of peak sound pressure level at the fundamental frequency in the vertical centerline plane at three positions aft of the trailing edge of an oscillating two-dimensional flat plate. f = 20 Hz.; $\alpha = 12^{\circ}$; $\Delta\alpha = \pm 3^{\circ}$.

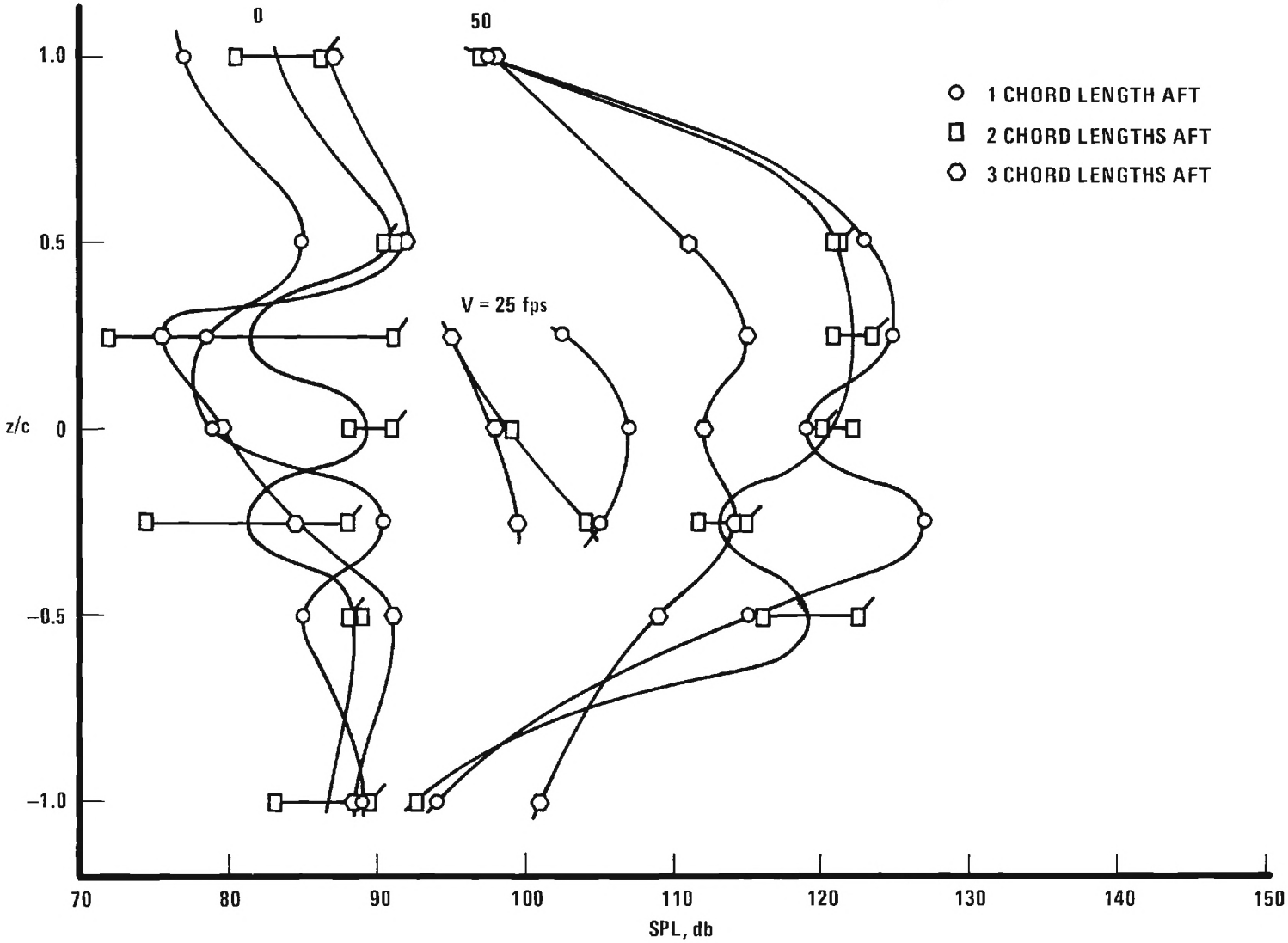

Figure 27. Variation of peak sound pressure level at first harmonic of the fundamental frequency in the vertical centerline plane at three positions aft of the trailing edge of an oscillating, two-dimensional flat plate. $f = 20$ Hz.; $\alpha = 12^{\circ}$; $\Delta\alpha = \pm 3^{\circ}$.

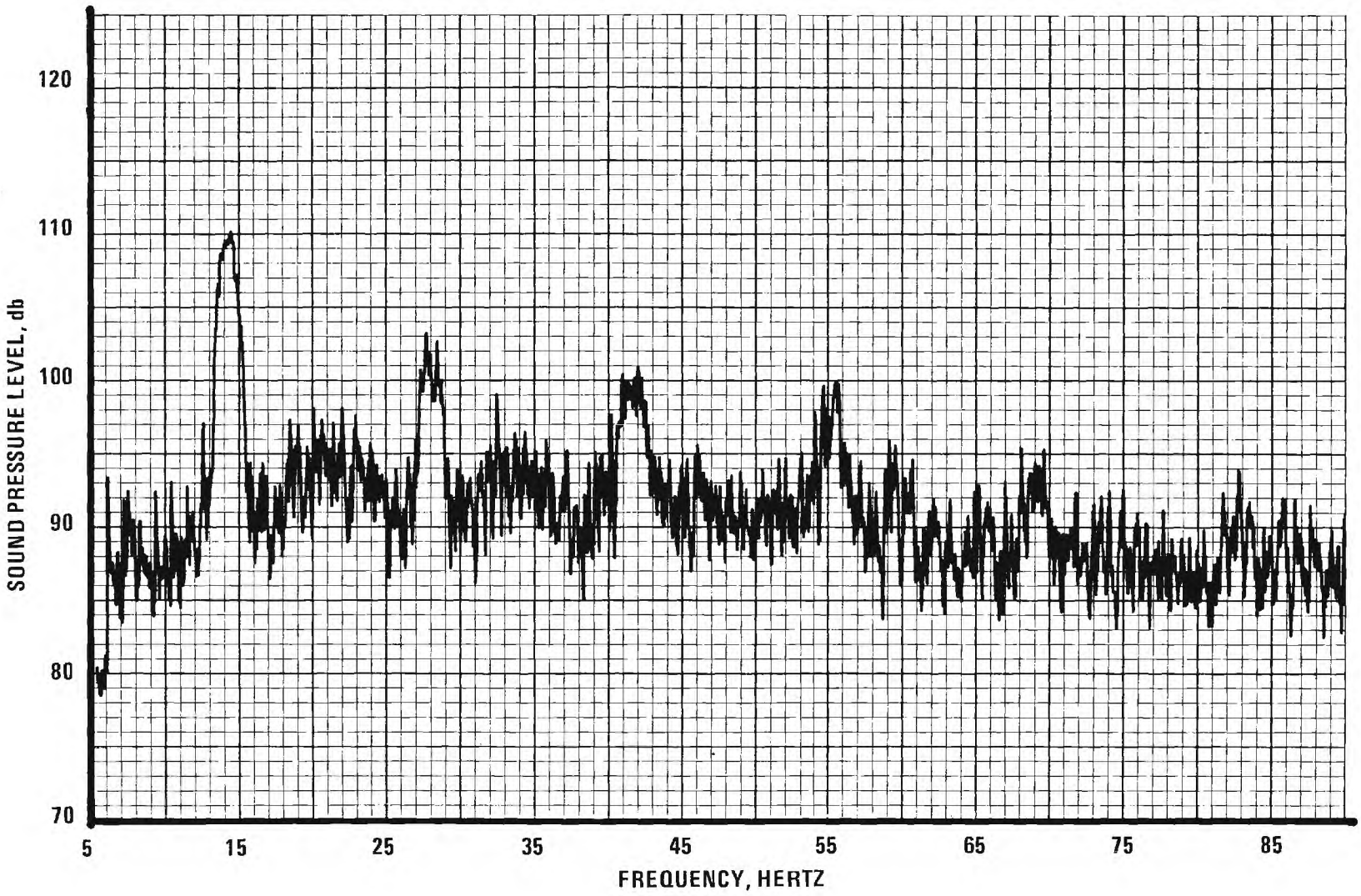

Figure 28. Sound pressure level in the wake of a flat plate oscillating at 14 Hz and airspeed of 25 FPS.